AJRCMB Articles in Press. Published on 20-December-2013 as 10.1165/rcmb.2013-0090OC

Cigarette Smoke-Induced Disruption of Bronchial Epithelial Tight Junctions is Prevented by Transforming Growth Factor-Beta

Andrea C. Schamberger, Nikica Mise, Jie Jia, Emmanuelle Genoyer,

Ali Ö. Yildirim, Silke Meiners, and Oliver Eickelberg

Comprehensive Pneumology Center, Institute of Lung Biology and Disease, University Hospital, Ludwig-Maximilians-University and Helmholtz Zentrum München, Member of the German Center for Lung Research, Munich, Germany

*Running title:*TGF-beta prevents cigarette smoke-induced injury*

To whomcorrespondence should be addressed:Oliver Eickelberg, Comprehensive Pneumology Center, Ludwig-Maximilians-Universität and Helmholtz Zentrum München, Max-Lebsche-Platz 31, 81377 München, Germany,Tel.: 0049(89)31874666; Fax: 0049(89)31874661; Email: oliver.eickelberg@helmholtz-muenchen.de

"This article has an online data supplement, which is accessible from this issue's table of content online at www.atsjournals.org"

ABSTRACT

The airway epithelium constitutes an essential immunological and cytoprotective barrier to inhaled insults, such as cigarette smoke, environmental particles, or viruses. While bronchial epithelial integrity is crucial for airway homeostasis, defective epithelial barrier functioncontributes to chronic obstructive pulmonary disease (COPD). Tight junctions at the apical side of epithelial cell-cell contactsdetermine epithelial permeability. Cigarette smoke exposure, the major risk factor for COPD,is suggested to impair tight junction integrity; however,detailed mechanismsthereof remain elusive. Here, we investigated whether cigarette smoke extract (CSE) and transforming growth factor (TGF)-β1affectedtight junction integrity. Exposure of human bronchial epithelial cells (16HBE14o$^-$), as well as differentiated primary human bronchial epithelial cells (pHBECs),to CSE significantly disruptedtight junction integrity and barrier function. Specifically, CSE decreased transepithelial electrical resistance (TEER)and tight junction-associated protein levels. Zona occludens (ZO)-1 and -2 protein levels weresignificantly reduced and dislocated from the cell membrane, as observed by fractionation and immunofluorescence analysis. These findings were reproduced in isolated bronchi exposed to CSE*ex vivo*, as detected by qRT-PCR and immunohistochemistry. Importantly, combined treatment of 16HBE14o$^-$ cells or pHBECs with CSE and TGF-β1 restored ZO-1 and ZO-2 protein levels. TGF-β1 co-treatment restored not only membrane localization of ZO-1 and ZO-2 protein, but also prevented CSE-mediatedTEER decrease. In conclusion, CSE led tothe disruption of tight junctions of human bronchial epithelial cells, whileTGF-β1 counteracted this CSE-inducedeffect. Thus, TGF-β1may serve as a protective factor for bronchial epithelial cell homeostasis in diseases such as COPD.

AJRCMB Articles in Press. Published on 20-December-2013 as 10.1165/rcmb.2013-0090OC

KEYWORDS

Claudin, zonula occludens-1 (ZO-1), zonula occludens-2 (ZO-2), cigarette smoke, TGF-β1, airway epithelium, bronchial epithelial cells, COPD, ciliated cell, goblet cell

INTRODUCTION

Chronic obstructive pulmonary disease (COPD), the fourth leading cause of death worldwide(1), is induced by environmental exposure to noxious gases, particles,indoor fumes, pathogens, or most importantly, by active or passive exposure to cigarette smoke(2). COPD is characterized by progressive airflow limitation due to an abnormal inflammatory response and structural pathological remodelling of the lung to these environmental exposures (3). The airway epithelium represents the lung's first line of defense,therefore, its barrier function and integrity is tightly regulated to prevent epithelial and interstitial damage(4). Cigarette smoke exposure leads to damage and increased permeability of the airway epithelium, as recently demonstrated *in vitro* in human bronchial epithelial cells (5) andCOPD patients compared with non-smokers and smokers (6). Animal studies using tracer moleculeshave shown that the epithelial permeability increases after smoke exposure(7, 8). Interestingly, these changes in permeability were transient and reversible(9). As such, we sought to elucidate the mechanisms of epithelial permeability, particularly tight junction disassembly, in response to cigarette smoke exposure in the bronchial epithelium.

Tight junctions are located at the most apical side of epithelial cell-cell contacts and represent the major junctional components determining the permeability of an epithelial sheet. Tight junctions are critically involved in the exchange of ions, solutes, and cells that travel across paracellular spaces. Furthermore, tight junctions regulate the formation of apico-basal polarity and control proliferation, gene expression, or cell differentiation through signaling pathways that are activated by tight junction components (10). More than 40 different proteins have been identified to be associated with tight junctions (11): Occludin (OCLN) and claudins (CLD), for example, are transmembrane spanning proteins forming the intercellular adhesions via hemophilic and heterophilic interactions. Zonula occludens-1 (ZO-1), ZO-2, ZO-3, cingulin, or MAGI-1 are located intracellularly and anchortransmembrane proteins with the actin cytoskeleton (10).

Cigarette smoke contains a complex mixture of about 4800 chemicals (12), making it difficult to define the cellular mechanisms that lead to smoking-related features of COPD in general and of injury of the airway epithelium in particular. A recent study demonstrateda transient decrease in airway epithelial barrier function inbronchial epithelial cells (13). In addition, human adenocarcinoma Calu-3 cells exposed to mainstream smoke exhibited decreased transepithelial electrical resistance (TEER), resulting from a highly regulated, yet undefined process not due to cytotoxicity of cigarette smoke(14). Downregulation of apical tight junction components, including claudins, was observed in chronic exposures of bronchial epithelial cells to cigarette smoke extract (CSE)(15, 16).

AJRCMB Articles in Press. Published on 20-December-2013 as 10.1165/rcmb.2013-0090OC

The multifunctional cytokine transforming growth factor-beta (TGF-β) exhibits immunosuppressive capacity and is produced by virtually all cell types in the lung (17). TGF-β receptor activation leads to subsequent phosphorylation of Smad2/3, complex formation with Smad4, and translocation to the nucleus, in turn regulatingtranscriptional activation and/or repression of selected target genes. Smad-dependent signaling can be inhibited by Smad6 or7, both inhibitory Smad isoforms, which are activated by e.g. IFN-γ or TNF-α stimulation. TGF-β is thought to significantly contribute to the pathogenesis of COPD(18), but its pleitropic actions make it difficult to assign distinct cellular functions during disease pathogenesis. For instance, smokers or ex-smokers with COPD revealed augmented TGF-β1 expression levels in bronchiolar epithelial cells (19). In contrast, a single-nucleotide-polymorphism (SNP) within the first exon of the TGF-β gene (reference SNP ID 1982073),which is associated with increased TGF-β levels,is more frequent in control and smoke-resistant subjects than COPD patients, suggesting that TGF-β could also have a protective role in COPD(20). In accordance with this notion, studies of intestinal epithelial cells have recently shown that TGF-β is also able to rescue epithelial barrier function(21-25). While TEER is increased in colon-derived epithelial cells treated with TGF-β(22, 23, 25), disruption of the intestinal epithelial barrier is counteracted by TGF-β(21-24). In addition, TGF-β blocked*Escherichia coli*-induced increased permeability via maintenance of claudin-2, occludin, and ZO-1 levels in intestinal epithelial cells(25), highly suggesting cell-specific effects of TGF-β function on epithelial integrity.

Accordingly, we hypothesized that TGF-β exerted protective functionson the bronchial epithelium exposed to cigarette smoke. To this end, we characterized the regulation and function of tight junctions and the role of TGF-β in response to cigarette smoke-induced epithelial barrier dysfunction. Our data demonstrate that bronchial epithelial barrier function was impaired, due to tight junction disintegration, when exposed to non-toxic doses of CSE and that TGF-β was able to prevent these changes. Importantly, understanding these mechanisms in greater detail will facilitate controlled regeneration of dysfunctional epithelial permeability to restore lung epithelial barrier function and integrity in diseases such as COPD.

MATERIAL AND METHODS

Cells Culture and Treatment

The 16HBE14o$^-$ human bronchial epithelial cell line was cultured in MEM media (PAA-Laboratories; Pasching, Austria) supplemented with 10% fetal bovine serum (FBS). If not stated otherwise, cells were seeded at a density of 2x10^4 cells/cm^2 and treated 48 hours later. Cigarette smoke extract (CSE) and/orTGF-β1 (R&D; Minneapolis, MN) treatment was performed every 24 hours.Chronic treatment was performed as shown in Supplemental Figure E4A.Normal human primary bronchial epithelial cells (Lonza; Wokingham, UK) were expanded in BEGMmedia (Lonza). Cells were seeded at passage 2-3 at a density of 1×10^4 cells/cm^2 and treated when confluent. For differentiation, cells were seeded at passage 2 at a density of 1×10^5 cells/cm^2 on human placental collagen type IV-coated (Sigma-Aldrich; St. Louis, MO) transwell inserts (transparent, 0.4 µm; Greiner; Solingen, Germany) in BEGM media. Cells were lifted to air-liquid interface (ALI)when confluent, apical media was then aspiratedand basolateral media substituted with PneumaCult™-ALI media (Stemcell Technologies; Köln, Germany) and changed every other day. If not stated otherwise, cells were treatedat day 14 after air-lift either withCSE (apical, 80µl) and/or TGF-β1 (apical and basolateral). The extent of differentiation wasquantified using Imaris 7.4.0 software (Bitplane; Zurich, Switzerland). Z-stack images of stained cultures were obtained by confocal microscopy (LSM710 system; Carl Zeiss; Oberkochen, Germany) and 1500 – 3500 cells per image were analyzed for positivity of differentiation makers. n = 10 images per group and time point were processed.

Preparation of CSE

100% CSE was generated as previously described (26). For details, see the online data supplement.

Cytotoxicity Assays

For details, see the online data supplement.

Transepithelial Electrical Resistance (TEER) Measurements

16HBE14o$^-$ cells: 1×10^5 cells/cm^2 were seeded onto rat-tail collagen typeI or human-placental collagen type IV(Sigma-Aldrich) -coated (10 µg/cm^2) 12-well transwell inserts (transparent, 0.4 µm; Greiner) with 500 µl apical and 1500 µl basolateral volumes. TEER was monitored using a Millcell-ERS-2 (Millipore; Billerica, MA) volt-ohm-meter. Cells were treated at indicated time points with CSE (apical) and/or TGF-β1 (apical and

AJRCMB Articles in Press. Published on 20-December-2013 as 10.1165/rcmb.2013-0090OC

basolateral),and TEER was assessed at the indicated time points. For TEER assessment in differentiated pHBECs, 500 µl BEGM media was added to the apical compartment.

Cell Fractionation and Western Blot Analysis

For details, see the online data supplement.

Cigarette Smoke Exposure of Isolated Airways

Airways were isolated from healthy female C57BL/6 mice (Charles River Laboratories; Sulzfeld, Germany)(27), washed, and incubated in CSE (6 samples each) for 2 hours on 6-well transwell inserts (Greiner). Apical media was transferred to the basal compartment and airways cultured on air-liquid-interface for additional 4 or 22 hours. For analysis, airways were embedded twice with 2% agarose medium and once with paraffin for immunohistochemistry,or frozen in liquid nitrogen for subsequent RNA isolation.

RNA Isolation and Quantitative Real-Time PCR (qRT-PCR) Analysis

For details, see the online data supplement. For specific gene amplification, primers listed in Table 1 were used.

Immunofluorescence and Immunohistochemistry Analysis

Immunostaining of cells (28)and paraffin sections (3 µm) (29)were performed as described previously.

RESULTS

Cigarette Smoke Extract Decreases Barrier Function in Bronchial EpithelialCells

In order to identify non-toxic doses of cigarette smoke extract (CSE), we treated normal human bronchial epithelial 16HBE14o-cells with a range of CSE concentrations for 24, 48, or 72 hours, and assessed cell viability by MTT assay (Figure 1A). As shown, 10% CSE was well tolerated by bronchial cells for up to 3 days of exposure. In contrast, 25% CSE significantly reduced cell viability after 24 hours, which was further exacerbated with prolonged CSE treatment. Importantly, 50% and 100% CSE induced pronounced cell death, as early as 24 hours after exposure. Similar results were obtained by FACS analysis using PI/Annexin V staining (Supplemental Figure E3B).16HBE14o- cell morphology was not significantly changed after 24 hours of CSE stimulation using non-toxic doses (Figure 1B). Of note, sensitivity of 16HBE14o- cells to CSE was strongly dependent on cell confluence. 25% CSE had no influence on cell viability in confluent cultures (Supplemental Figure E1).Exposure of bronchial epithelial cells to 10% CSE for 6 hours significantly decreased transepithelial electrical resistance (TEER) compared with control (NT) conditions (Figure 1C). This effect was enhanced using 25% CSE. These data demonstrate that CSE specifically impairs barrier function *in vitro* in normal bronchial epithelial cells, as early as 6 hours after exposure to non-toxic doses of CSE.

CSE-Induced Barrier Dysfunction Involves Downregulation of Tight Junction Molecules

To elucidate the mechanisms of CSE-induced barrier dysfunction, we investigated the expression and localization of cell-cell adhesion components. Bronchial epithelial cells were exposed for 2 or 24 hours to 10% CSE and levels of the tight junction molecules ZO-1, ZO-2, OCLN, CLD-4, and CLD-6 were analyzed by Western blot analysis (Figure 2A and 2B). CSE exposure significantly diminished ZO-1 protein levels within 2 hours. Protein levels of ZO-2 and OCLN were significantly reduced after 2 hours, albeit to a lesser extent, but fully recovered within 24 hours. In contrast, decreased protein levels of both, CLD-4 and CLD-6, were observed after 24 hours of CSE injury.The mRNA levels of tight junction proteins did not change within 24 hours of CSE treatment (Supplemental Figure E2), indicating post-transcriptional or post-translational regulation of tight junction proteins in response to CSE. To further investigate this issue, we performed immunofluorescence staining for ZO-1, ZO-2, or OCLN of 16HBE14o- cells treated with or without 10% CSE for 72 hours (Figure 2C). Control cells demonstratedcontinuous membrane localization of ZO-1 expression. Additional fractionation analysis (Figure 2D) confirmed that ZO-1 protein was mainly present in the membrane fraction of unstimulated cells. Upon CSE exposure, continuous staining of ZO-1 was disrupted and appeared as a discontinuous and

AJRCMB Articles in Press. Published on 20-December-2013 as 10.1165/rcmb.2013-0090OC

fragmented, demonstrating disruption of tight junctions (Figure 2C). In accordance with this observation, ZO-1 protein decreased in the membrane fraction,as early as 2 hours after CSE treatment, and was detected in the cytoplasmic fraction (Figure 2D). Membrane-associated ZO-1 protein levels were significantly diminished by ~50% within this time period, as quantified by densitometry analysis using Na^+/K^+-ATPase as a membrane marker. Furthermore, staining for ZO-2 and OCLN (Figure 2C) resembled the staining of ZO-1 in control, as well as in CSE-exposed cells. Taken together, these results indicate that tight junction integrity is impaired by CSE via downregulation of tight junction components, particularly by loss of ZO proteins from the membrane.

CSE Decreases ZO-1 levels in Mouse Airways

To assess whether these *in vitro* effects were also observed in controlled exposures of intact bronchi, we performed an *ex vivo* analysis of mouse airways exposed to CSE. Mouse airways were incubated in control medium, 5%, 10%, or 20% CSE for 2 hours under submerged conditions. Subsequently, bronchi were transferred to ALI culture conditions in the presence of the same treatment mediaprovided on the basal side. Upon exposure to CSE, ZO-1 transcript levels were significantly diminished in a time- and concentration-dependent manner (Figure 3A). In control airways, continuous apical staining of ZO-1 (red) between bronchial epithelial cells was observed by immunohistochemical analysis (Figure 3B), suggesting well-preserved tight junctions in controlisolated airways. In contrast, we observed a striking difference in ZO-1 organization in CSE-exposed airways: ZO-1 staining was markedly reduced after CSE exposure for 24 hours, indicating disruption of junctional integrity. This finding was fully supportive of our *in vitro* results and indicated that CSE decreased tight junction components in bronchial epithelial cells both *in vitro* and*ex vivo*.

TGF-β1 Counteracts CSE-Induced Barrier Dysfunction by Upregulation of Junctional Components

TGF-β has been reported to improve, as well as decrease epithelial barrier function, depending on the organ and microenvironment investigated. As such, we investigated the influence of TGF-β1 alone or in combination with CSE on bronchial epithelial cell junctional integrity. Cells were treated with TGF-β1 at the indicated concentrations for 24 hours, after which ZO-1 and ZO-2 protein levels were assessedby Western blot analysis (Figure 4A). All concentrations of TGF-β1 used increased ZO-1 and ZO-2 protein levels, with concomitant phosphorylation of Smad3 (pSmad3). Next, cells were treated for 2 and 24 hours with TGF-β1, CSE (2.5% and 10%), or a combination thereof(Figure 4B). After 2 hours, ZO-1 and ZO-2 protein levels were clearly downregulated in CSE-treated cells compared with control (NT), as depictedin Figure 2. Remarkably, TGF-β1 treatment protected bronchial epithelial cells from CSE-mediated downregulation of tight junction

proteins(Figure 4B). Interestingly, OCLN levels were not affected by TGF-β1 treatment. These findings were still evident 72 hours after treatment with 10% CSE or 10% CSE+TGF-β1, as demonstrated by immunofluorescence analysis (Figure 4C). While membrane staining of ZO-1 and ZO-2 was disrupted by CSE treatment, addition of TGF-β1 prevented this effect and demonstrated continuous membrane staining of ZO-1 and ZO-2 at cell boundaries, mimicking the expression pattern of unstimulated cells.

To assess whether TGF-β1 is also able to functionally protect against CSE-induced barrier dysfunction, TEER of cells co-stimulated with CSE and TGF-β1 was measured (Figure 4D and 4E). Cells were plated on collagen I-coated (Figure 4D) or collagen IV-coated (Figure 4E) transwell inserts. Exposure to CSE clearly decreased TEER levels in both settings, while TGF-β1 alone did not change TEER levels compared with control. Of note, TGF-β1 co-treatmentprotected bronchial epithelial cells from CSE-induced barrier dysfunction. This effect was even more evident, when cells were plated on collagen IV.To investigate whether TGF-β1 exerted its protective effect by increasing proliferation or cell survival, BrdUincorporation assay and PI/Annexin-V staining were performed, respectively (Supplemental Figure E3). Cells treated for 24 and 72 hours with 10% CSE + TGF-β1 demonstrated aslight decrease inproliferation compared to CSE-treated cells (Supplemental Figure E3A). Further, TGF-β1 treatment did not affect apoptosis/necrosis ratios of the cells (Supplemental Figure E3B).

Interestingly, we did not identify any changes in transcript levels of tight junction components within 24 hours of treatment with TGF-β1 or TGF-β1 combined with CSE (Supplemental Figure E2). In order to analyze whether TGF-β1 affects transcriptional regulation of tight junction proteins after chronic exposure with CSE, cells were chronically treated and RNA levels analyzed by qRT-PCR (treatment scheme is pictured inSupplemental Figure E4A). To control for effective responses ofbronchial epithelial cells to TGF-β1, the expression oftwo TGF-β1 target genes, fibronectin and SNAIL was analysed. Both markers were markedly elevated by TGF-β1, as well as by TGF-β1 in combination with CSE (Supplemental Figure E4B). Next, we sought to investigate how the expression of different junctional components is affected by TGF-β1 treatment (Figure 5). Of note, TGF-β1 induced concerted upregulation of several junctional proteins such as ZO-1, ZO-2, CLD4, and CLD6 by up to 1.5 fold with OCLN and E-cadherin (Supplemental Figure E4B) transcript following the same trend. When cells were treated with a combination of TGF-β1 and CSE, very similar effects could be observed: ZO-2, CLD4, and CLD6 mRNA levels were significantly augmented in cells treated with both TGF-β1 and CSE. Furthermore, ZO-1 and OCLN mRNA levels followed the same trend.

AJRCMB Articles in Press. Published on 20-December-2013 as 10.1165/rcmb.2013-0090OC

TGF-β1 Exerts its Protective Effect in CSE-treated Differentiated Primary Human Bronchial Epithelial Cells

To assess whether TGF-β1 can also counteract CSE-induced barrier dysfunction in primary human bronchial epithelial cells (pHBECs), we investigated two different settings:pHBECs were either cultured on plastic (non-differentiated) or at the air-liquid interface (ALI) to achieve mucociliary differentiation.Effective differentiation wasconfirmed by immunofluorescence staining (Figure 6A) and quantification of differentiation makers (Figure 6B) over time. ZO-1 expression was present already 7 days after air-lift and increased further until 21 days. Acetylated-tubulin (ciliated cells), clara cell specific protein (clara cells) and Mucin 5AC (goblet cells)were expressed only on the apical side (Supplemental Figure E6) and increased markedly over time. Of note, we also found some cells stained double positive for Muc5AC and CC10 after 21 days of differentiation (8.6%), while no cells were double positive for acetylated-tubulin and CC10.Basal cells, positive for p63, were only found in the most basal cell layer (Supplemental Figure E6).

To identify non-toxic doses of CSE,pHBECs were treated with a range of CSE concentrations for up to 72 hours and LDH assay was performed (Supplemental Figure E5A). Up to 10% CSE did not trigger any LDH release from the cells, while 25% CSE was toxic in prolonged treatment for non-differentiated cells. Differentiated pHBECs proved to be even more resistant to 25% CSE(Supplemental Figure E5B).Next, we investigated whether CSE hadsimilar effects on ZO-1 and ZO-2 expression levels in pHBECs, as observed with 16HBE14o$^-$ cells.After 24 hours of CSE exposure, we observed decreased ZO-1 and ZO-2 levels in a concentration-dependent manner(Figure 7A). Interestingly, ZO-1 and ZO-2 protein levels of differentiated cultures were clearly diminished after 72 hours of CSE exposure(Figure 7B).This might indicate higher resistance ofdifferentiated cells to CSE injury.Moreover, differentiated pHBECs stimulated with 10% CSE for 72 hours demonstrated disrupted and/or zipper-like junctional appearance compared to control cells (Figure 7C). This result was further corroborated by TEER decrease after 10% and 25% CSE (Figure 7D). To test whether TGF-β1 treatment increased the expression of tight junction proteins in pHBECs, cells weretreated with a range of TGF-β1 concentrations and ZO-1 and ZO-2 levels analyzed by Western blot.Again, phosphorylated Smad3 served as a positive control for TGF-β1 response(Figure 7A). After 24 hours of treatment, both ZO-1 and ZO-2 protein levels were increased in a concentration-dependent manner. No differences in ZO-1 and ZO-2 levels were observed in differentiated pHBECs, when treated withdifferentTGF-β1 concentrations (Figure 7B).

Finally, we were interested whether TGF-β1 had the capacity to prevent CSE-induced injuryin pHBECs. As demonstrated in Fig. 7A, TGF-β1 protected pHBECs from CSE-mediated downregulation of ZO-2 protein. Of note, these findings were also evident in differentiated pHBECs (Figure 7B), when treated for 72 hours with

TGF-β1, 10% CSE, or 10% CSE + TGF-β1. While 10% CSE decreased ZO-1 and ZO-2 protein levels, addition of TGF-β1 prevented this effect.These results were functionally reflected in TEER measurements, as co-stimulation with CSE and TGF-β1 for 6 hours had a clear protective effect on loss of resistance compared to CSE only (Figure 7D). In accordance to our previous results, the protective effect of TGF-β1 was also evident in differentiated pHBECs.

AJRCMB Articles in Press. Published on 20-December-2013 as 10.1165/rcmb.2013-0090OC

DISCUSSION

The bronchial epithelium is responsible for preserving airway homeostasis in the lung. It possesses innate defense functions and acts as a barrier against inhaled particles or pathogens. Epithelial barrier function is maintained by adherens junctions and, most importantly, by intercellular tight junctions. Here, we show that acute CSE exposureimpairedthe barrier function of human bronchial epithelial cells. We also provide evidence that tight junction components werespecifically affected by smoke injury. In particular, ZO-1 was displaced from the membrane fraction, contributing to severe tight junction disintegrity. Importantly, disruption of tight junctions with a loss of tight junction proteins from the membrane was confirmed in an *ex vivo* mouse model. Finally, TGF-β was able to prevent CSE-induced disruption of tight junction in human bronchial epithelial cells and preserve their barrier function.

While the cytotoxic effects of cigarette smoke and its*in vitro* surrogate CSE on bronchial epithelial cells are well established, the mechanisms of cigarette smoke-induced impairment of bronchial epithelial barrier function are less well understood. Here, we analyzed the effects of CSE on tight junctions:*in vitro* using the human bronchial epithelial cell line 16HBE14o$^-$, as well as primary human bronchial epithelial cells (pHBEC),and *ex vivo* using cultures of isolated mouse airways. While 100% and 50% CSE induced acute cell death of bronchial epithelial cells, 10% prolonged CSE exposure neither decreased cell viability over long time-periods, nor affected cell morphology. Differentiated pHBECs proved even more resistant to CSE compared with 16HBE14o- cells and non-differentiated pHBECs. Importantly, resistance measurements of 16HBE14o$^-$monolayers (TEER) revealed a dose-dependent impairment of barrier function within 6 hours of CSE exposure (CSE doses of 10% and 25%), consistent with previous reports (13, 15, 30). As such, the regulation of barrier function by cigarette smoke is a specific effect and not simply due to toxic effects. As intact barrier function strongly depends on intact tight junctions, we studied the effects of smoke on tight junction proteins with respect to RNA and protein expression and subcellular localization.

Tight junction components, such as occludin, claudins,orjunctional adhesion molecules (JAMs), are linked to the actin cytoskeleton by ZO proteins, thereby enabling these proteins to constitute major stabilizing factors of tight junctions. Accordingly, ZO proteins have been shown to be essential for tight junction formation (31).In the current study,we observed a pronounced and acute loss of membrane associated ZO-1 after CSE exposure. Similarly, ZO-2 and occludin protein amounts were significantly decreased after CSE treatment, while claudin-4 and claudin-6 showed delayed downregulation. Thus, junctional integrity was disrupted by CSE exposure.Importantly, pHBECs showed a very similar response to CSE injury. In both, non-differentiated and

differentiated cultures, we observed a striking downregulation of ZO-1 and ZO-2 protein levels when exposed to CSE. In agreement with our results, Heijink et al.(13) described delocalization of tight junction proteins from the junctions *in vitro*after 4 hours of CSE exposure. This goes in line with an earlier report from Petecchia et al.(32), where ZO-1 staining decreased in a time- and concentration-dependent manner in CSE-stimulated bronchial epithelial cells.

In an *ex vivo* mouse model, we could confirm that CSE exposure had the capacity to reduce ZO-1 also in fully intact mouse airways. The discrepancy that RNA levels of junctional components were only affected in the *ex vivo* model and not in the cell lines, could be explained by the existing microenvironment in the *ex vivo* model and the different origins of the cells. Our finding that a tight junction protein (ZO-1) is diminished in murine bronchi upon exposure to CSE is novel and shows for the first time the direct effect of cigarette smoke on a tight junction component *ex vivo*.

It is tempting to speculate that reduced ZO-1 expression is the underlying mechanism for the smoke-induced barrier dysfunction also reported*in vivo*(6, 8, 9). This notion is supported by findings in ZO-1/ZO-2 depleted mammary epithelial cells, reporting an inability to form tight junctions and epithelial resistance, as measured by TEER(31). In contrast, knockout of ZO-1 resulted in delayed tight junction and barrier formation (33), because of a compensatory increase of ZO-2. The concerted decrease of ZO-1 and ZO-2,which we found in CSE-exposed cells,might havesimilar effects:neither protein is able to compensate for the other, resulting in tight junction disintegrity.The central role of ZO-1 proteins in tight junction stability is also reflected by the fact thatZO-1 proteins are key for initiation of tight junction formation. ZO-1 is known to first colocalize with cadherins in spot-like adherens junctions. These gradually fuse to form mature, belt-like junctions, and recruit claudins/occludin for tight junction polymerization (33). As soon as tight junctions are finally separated from adherens junctions in well polarized cells, ZO-1 is exclusively concentrated at tight junctions.This proposes thatloss of ZO-1 and ZO-2 due to cigarette smokeleads to destabilization of the junctions, because polymerization of newly synthesized claudin and occludin is impaired.Claudin or occludin proteins that are already polymerized at tight junctions are probably not directly affected by the loss of ZO proteins. This is indicated by the observation that protein levels of claudins and occludin remained unchanged and localized normally to the tight junctions in ZO-1/ZO-2 depleted cells (31). Besides ZO-1, occludin has been reported to play a central role in tight junction stability and barrier function (34). Thus, its defect by cigarette smoke is most likely directly coupled to the resistance decrease found after cigarette smoke exposure.

Interestingly, downregulation of ZO-1 in bronchial epithelial cells was already observed after 2 hours of CSE exposure and still evident after 72 hours, as observed by membrane fractionation and immunofluorescence

AJRCMB Articles in Press. Published on 20-December-2013 as 10.1165/rcmb.2013-0090OC

staining. As RNA levels were not affected, these data strongly point towards an acute and post-translational regulation of membrane-associated ZO-1 proteins by cigarette smoke, such as membrane distraction and degradation. Heijink et al. suggested that tight junction proteins are cleaved by calpains and lost from the membrane in response to cigarette smoke (13). For other membrane bound proteins such as the EGF-, VEGF-, and interferon-γ receptor, it has been shown that cigarette smoke oxidatively modified these proteins, thereby priming them for membrane distraction and degradation by the ubiquitin proteasome system (35-38). The delayed downregulation of claudins by CSE that we have observed may have different reasons. First, claudins have a much longer half-life than occludin (39), which mayprotect these from CSE-dependent degradation, as long as they are integrated within the junctional complex. Second, there is possibility that the CSE-dependent degradation of claudins follows a different time course through different proteolytic pathways, than the degradation of ZO-1, ZO-2, and occludin, and is therefore delayed.

TGF-β is known to play important roles in chronic lung disease. It is still unclear, however, if this multifunctional cytokine is protective or supportive to the pathogenesis of COPD. Herein, we found clear evidence that TGF-β1 protects from the disrupting effect of CSE on tight junctions. Both ZO-1 and ZO-2 were protected from membrane loss upon exposure to CSE, when bronchial epithelial cells were co-treated with TGF-β1. Only 2 hours of TGF-β1 stimulation prevented CSE-induced loss of tight junction proteins and 24 hours of combined treatment with CSE and TGF-β1 even enhanced protein levels of ZO-1 and ZO-2, compared with controls. This effect was specific for ZO-1 and ZO-2, as occludin levels were not markedly enhanced upon TGF-β1 stimulation. Furthermore, junctional integrity could be maintained in bronchial cells, when co-treated with both, CSE and TGF-β1, as observed by belt-like ZO-1 and ZO-2 immunofluorescence staining pattern resembling the localization of intact junctions of untreated cells.In addition, pHBECs exhibted a very similar response to TGF-β1 stimulation. In both, non-differentiated and differentiated cultures, TGF-β1 prevented downregulation of ZO-2 protein levels, when co-treated with CSE. Importantly, we also provide functional evidence that TGF-β1 prevented CSE-dependent loss of barrier function (TEER) in a dose dependent manner. In line with our study,TGF-β has been shown to enhance epithelial barrier function in intestinal cells and to rescue barrier disruption caused by *Cryptosporidium parvum*, IFN-γ, or Enterohemorrhagic *Escherichia coli* O157:H7 (21-25). Besides TGF-β, epidermal growth factor (EGF) has also been associated with tight junction protection in injured intestinal cells (40). This concept of barrier protection via EGF has recently been transferred to the lung field: EGFR positively regulates permeability barrier development through the Rac1/JNK-dependent pathway (41). Moreover, EGF treatment restored tight junctions in epithelial cultures from asthmatic subjects (42). As such, we can speculate on the mechanisms of the protective effect of TGF-β, which may explain how

airway epithelial cells circumvent the deleterious effects of CSE on tight junction integrity: TGF-β1 is endogenously released upon smoke exposure, possibly as a protective mechanism *in vivo*(19, 43), and increased TGF-β1-activity downregulates proteasomal activity in lung A549 cells(44). Potentially, TGF-β1 therefore counteracts proteasomal degradation of tight juntion components by the proteasome, a degradation pathway previously reported to control ZO-1 and -2 levels during tight junction disintegration (45). The capability of TGF-β1 to diminish the downregulation of ZO-1 and ZO-2 protein levels after only 2 hours can only be explained by post-translational regulation, as no changes on transcript levels were observed within 24 hours of TGF-β1 stimulation. Only E-cadherin mRNA levels were found to be significantly increased within 24 hours of TGF-β1 stimulation. Since co-localization of ZO proteins with cadherins are key for tight junction formation(33), and E-cadherin expression is crucial for proper tight junction architecture and epithelial resistance(46, 47), upregulation of E-cadherin by TGF-β1 might help to stabilize tight junctionsafter CSE exposure. Interestingly, upregulation of ZO-1, ZO-2, claudin-4,or claudin-6 mRNA levels could be observed at later time points, when cells were stimulated with TGF-β1 in combination with CSE.This strengthens the hypothesis that TGF-β1 not only protects, but also counter-regulates the loss of tight junction proteins after injury.

Taken together, we show that CSE disrupted tight junction integrity in human bronchial epithelial cells. Importantly, similar results have been observed using an *ex vivo* mouse model. TGF-β1 prevented CSE-induced tight junction disruption and loss of barrier function. Since our data resemble molecular processes that largely occur after acute exposure to CSE, we speculate that protective spatiotemporal effects of TGF-β on the bronchial epithelium may play an important role in maintaining epithelial cell homeostasis, possibly preventing pathological remodeling in diseases such as COPD.

AJRCMB Articles in Press. Published on 20-December-2013 as 10.1165/rcmb.2013-0090OC

ACKNOWLEDGMENTS

We thank Ann-Christin Beitel and Daniela Dietel for excellent technical assistance and Dr. Otmar Schmid (iLBD) for valuable discussion.

REFERENCES

1. WHO. World health statistics 2008. 2008 [cited 2012 Sep 11]. Available from: http://www.who.int/whosis/whostat/EN_WHS08_Full.pdf.
2. Decramer M, Janssens W, Miravitlles M. Chronic obstructive pulmonary disease. *Lancet* 2012;379(9823):1341-1351.
3. Global initiative for chronic obsructive lung disease. Global strategy for the diagnosis, management, and prevention of copd: Updated 2010. 2010 [cited 2012 Sep 12]. Available from: http://www.goldcopd.org/uploads/users/files/GOLDReport_April112011.pdf.
4. Li XY, Rahman I, Donaldson K, MacNee W. Mechanisms of cigarette smoke induced increased airspace permeability. *Thorax* 1996;51(5):465-471.
5. Rusznak C, Mills PR, Devalia JL, Sapsford RJ, Davies RJ, Lozewicz S. Effect of cigarette smoke on the permeability and il-1beta and sicam-1 release from cultured human bronchial epithelial cells of never-smokers, smokers, and patients with chronic obstructive pulmonary disease. *Am J Respir Cell Mol Biol* 2000;23(4):530-536.
6. Jones JG, Minty BD, Lawler P, Hulands G, Crawley JC, Veall N. Increased alveolar epithelial permeability in cigarette smokers. *Lancet* 1980;1(8159):66-68.
7. Burns AR, Hosford SP, Dunn LA, Walker DC, Hogg JC. Respiratory epithelial permeability after cigarette smoke exposure in guinea pigs. *J Appl Physiol* 1989;66(5):2109-2116.
8. Simani AS, Inoue S, Hogg JC. Penetration of the respiratory epithelium of guinea pigs following exposure to cigarette smoke. *Lab Invest* 1974;31(1):75-81.
9. Hulbert WC, Walker DC, Jackson A, Hogg JC. Airway permeability to horseradish peroxidase in guinea pigs: The repair phase after injury by cigarette smoke. *Am Rev Respir Dis* 1981;123(3):320-326.
10. Guillemot L, Paschoud S, Pulimeno P, Foglia A, Citi S. The cytoplasmic plaque of tight junctions: A scaffolding and signalling center. *Biochim Biophys Acta* 2008;1778(3):601-613.
11. Gonzalez-Mariscal L, Betanzos A, Nava P, Jaramillo BE. Tight junction proteins. *Prog Biophys Mol Biol* 2003;81(1):1-44.
12. Baum SL, Andreson IGM, Baker RR, Murphy DM, Rowlands CC. Electron spin resonance and spin trap investigation of free radicals in cigarette smoke: Development of a quantification procedure. *Anal Chim Acta* 2003;481(1):1-13.

AJRCMB Articles in Press. Published on 20-December-2013 as 10.1165/rcmb.2013-0090OC

13. Heijink IH, Brandenburg SM, Postma DS, van Oosterhout AJ. Cigarette smoke impairs airway epithelial barrier function and cell-cell contact recovery. *Eur Respir J* 2012;39(2):419-428.
14. Olivera DS, Boggs SE, Beenhouwer C, Aden J, Knall C. Cellular mechanisms of mainstream cigarette smoke-induced lung epithelial tight junction permeability changes in vitro. *Inhal Toxicol* 2007;19(1):13-22.
15. Shaykhiev R, Otaki F, Bonsu P, Dang DT, Teater M, Strulovici-Barel Y, Salit J, Harvey BG, Crystal RG. Cigarette smoking reprograms apical junctional complex molecular architecture in the human airway epithelium in vivo. *Cell Mol Life Sci* 2011;68(5):877-892.
16. Veljkovic E, Jiricny J, Menigatti M, Rehrauer H, Han W. Chronic exposure to cigarette smoke condensate in vitro induces epithelial to mesenchymal transition-like changes in human bronchial epithelial cells, beas-2b. *Toxicol In Vitro* 2011;25(2):446-453.
17. Coker RK, Laurent GJ, Shahzeidi S, Hernandez-Rodriguez NA, Pantelidis P, du Bois RM, Jeffery PK, McAnulty RJ. Diverse cellular tgf-beta 1 and tgf-beta 3 gene expression in normal human and murine lung. *Eur Respir J* 1996;9(12):2501-2507.
18. Hogg JC, Timens W. The pathology of chronic obstructive pulmonary disease. *Annu Rev Pathol* 2009;4:435-459.
19. de Boer WI, van Schadewijk A, Sont JK, Sharma HS, Stolk J, Hiemstra PS, van Krieken JH. Transforming growth factor beta1 and recruitment of macrophages and mast cells in airways in chronic obstructive pulmonary disease. *Am J Respir Crit Care Med* 1998;158(6):1951-1957.
20. Wu L, Chau J, Young RP, Pokorny V, Mills GD, Hopkins R, McLean L, Black PN. Transforming growth factor-beta1 genotype and susceptibility to chronic obstructive pulmonary disease. *Thorax* 2004;59(2):126-129.
21. Planchon SM, Martins CA, Guerrant RL, Roche JK. Regulation of intestinal epithelial barrier function by tgf-beta 1. Evidence for its role in abrogating the effect of a t cell cytokine. *J Immunol* 1994;153(12):5730-5739.
22. Roche JK, Martins CA, Cosme R, Fayer R, Guerrant RL. Transforming growth factor beta1 ameliorates intestinal epithelial barrier disruption by cryptosporidium parvum in vitro in the absence of mucosal t lymphocytes. *Infect Immun* 2000;68(10):5635-5644.
23. Planchon S, Fiocchi C, Takafuji V, Roche JK. Transforming growth factor-beta1 preserves epithelial barrier function: Identification of receptors, biochemical intermediates, and cytokine antagonists. *J Cell Physiol* 1999;181(1):55-66.

24. McKay DM, Singh PK. Superantigen activation of immune cells evokes epithelial (t84) transport and barrier abnormalities via ifn-gamma and tnf alpha: Inhibition of increased permeability, but not diminished secretory responses by tgf-beta2. *J Immunol* 1997;159(5):2382-2390.

25. Howe KL, Reardon C, Wang A, Nazli A, McKay DM. Transforming growth factor-beta regulation of epithelial tight junction proteins enhances barrier function and blocks enterohemorrhagic escherichia coli o157:H7-induced increased permeability. *Am J Pathol* 2005;167(6):1587-1597.

26. van Rijt SH, Keller IE, John G, Kohse K, Yildirim AO, Eickelberg O, Meiners S. Acute cigarette smoke exposure impairs proteasome function in the lung. *Am J Physiol Lung Cell Mol Physiol* 2012.

27. Yildirim AO, Veith M, Rausch T, Muller B, Kilb P, Van Winkle LS, Fehrenbach H. Keratinocyte growth factor protects against clara cell injury induced by naphthalene. *Eur Respir J* 2008;32(3):694-704.

28. Mise N, Savai R, Yu H, Schwarz J, Kaminski N, Eickelberg O. Zyxin is a transforming growth factor-beta (tgf-beta)/smad3 target gene that regulates lung cancer cell motility via integrin alpha5beta1. *J Biol Chem* 2012;287(37):31393-31405.

29. Kneidinger N, Yildirim AO, Callegari J, Takenaka S, Stein MM, Dumitrascu R, Bohla A, Bracke KR, Morty RE, Brusselle GG, et al. Activation of the wnt/beta-catenin pathway attenuates experimental emphysema. *Am J Respir Crit Care Med* 2011;183(6):723-733.

30. Gangl K, Reininger R, Bernhard D, Campana R, Pree I, Reisinger J, Kneidinger M, Kundi M, Dolznig H, Thurnher D, et al. Cigarette smoke facilitates allergen penetration across respiratory epithelium. *Allergy* 2009;64(3):398-405.

31. Umeda K, Ikenouchi J, Katahira-Tayama S, Furuse K, Sasaki H, Nakayama M, Matsui T, Tsukita S, Furuse M, Tsukita S. Zo-1 and zo-2 independently determine where claudins are polymerized in tight-junction strand formation. *Cell* 2006;126(4):741-754.

32. Petecchia L, Sabatini F, Varesio L, Camoirano A, Usai C, Pezzolo A, Rossi GA. Bronchial airway epithelial cell damage following exposure to cigarette smoke includes disassembly of tight junction components mediated by the extracellular signal-regulated kinase 1/2 pathway. *Chest* 2009;135(6):1502-1512.

33. Umeda K, Matsui T, Nakayama M, Furuse K, Sasaki H, Furuse M, Tsukita S. Establishment and characterization of cultured epithelial cells lacking expression of zo-1. *J Biol Chem* 2004;279(43):44785-44794.

34. Cummins PM. Occludin: One protein, many forms. *Mol Cell Biol* 2012;32(2):242-250.

AJRCMB Articles in Press. Published on 20-December-2013 as 10.1165/rcmb.2013-0090OC

35. Meiners S, Eickelberg O. What shall we do with the damaged proteins in lung disease? Ask the proteasome! *Eur Respir J* 2012;40(5):1260-1268.

36. Dorofeyeva LV. Obtaining of measles virus haemagglutinin from strain l-16 grown in primary cell cultures. *Acta Virol* 1975;19(6):497.

37. HuangFu WC, Liu J, Harty RN, Fuchs SY. Cigarette smoking products suppress anti-viral effects of type i interferon via phosphorylation-dependent downregulation of its receptor. *FEBS Lett* 2008;582(21-22):3206-3210.

38. Khan EM, Lanir R, Danielson AR, Goldkorn T. Epidermal growth factor receptor exposed to cigarette smoke is aberrantly activated and undergoes perinuclear trafficking. *FASEB J* 2008;22(3):910-917.

39. Traweger A, Fang D, Liu YC, Stelzhammer W, Krizbai IA, Fresser F, Bauer HC, Bauer H. The tight junction-specific protein occludin is a functional target of the e3 ubiquitin-protein ligase itch. *J Biol Chem* 2002;277(12):10201-10208.

40. Samak G, Aggarwal S, Rao RK. Erk is involved in egf-mediated protection of tight junctions, but not adherens junctions, in acetaldehyde-treated caco-2 cell monolayers. *Am J Physiol Gastrointest Liver Physiol* 2011;301(1):G50-59.

41. Terakado M, Gon Y, Sekiyama A, Takeshita I, Kozu Y, Matsumoto K, Takahashi N, Hashimoto S. The rac1/jnk pathway is critical for egfr-dependent barrier formation in human airway epithelial cells. *Am J Physiol Lung Cell Mol Physiol* 2011;300(1):L56-63.

42. Xiao C, Puddicombe SM, Field S, Haywood J, Broughton-Head V, Puxeddu I, Haitchi HM, Vernon-Wilson E, Sammut D, Bedke N, et al. Defective epithelial barrier function in asthma. *J Allergy Clin Immunol* 2011;128(3):549-556 e541-512.

43. Takizawa H, Tanaka M, Takami K, Ohtoshi T, Ito K, Satoh M, Okada Y, Yamasawa F, Nakahara K, Umeda A. Increased expression of transforming growth factor-beta1 in small airway epithelium from tobacco smokers and patients with chronic obstructive pulmonary disease (copd). *Am J Respir Crit Care Med* 2001;163(6):1476-1483.

44. Ali A, Wang Z, Fu J, Ji L, Liu J, Li L, Wang H, Chen J, Caulin C, Myers JN, et al. Differential regulation of the reggamma-proteasome pathway by p53/tgf-beta signalling and mutant p53 in cancer cells. *Nat Commun* 2013;4:2667.

45. Nakamuta S, Endo H, Higashi Y, Kousaka A, Yamada H, Yano M, Kido H. Human immunodeficiency virus type 1 gp120-mediated disruption of tight junction proteins by induction of proteasome-mediated

degradation of zonula occludens-1 and -2 in human brain microvascular endothelial cells. *J Neurovirol* 2008;14(3):186-195.

46. Heijink IH, Brandenburg SM, Noordhoek JA, Postma DS, Slebos DJ, van Oosterhout AJ. Characterisation of cell adhesion in airway epithelial cell types using electric cell-substrate impedance sensing. *Eur Respir J* 2010;35(4):894-903.

47. Tunggal JA, Helfrich I, Schmitz A, Schwarz H, Gunzel D, Fromm M, Kemler R, Krieg T, Niessen CM. E-cadherin is essential for in vivo epidermal barrier function by regulating tight junctions. *EMBO J* 2005;24(6):1146-1156.

AJRCMB Articles in Press. Published on 20-December-2013 as 10.1165/rcmb.2013-0090OC

FOOTNOTES

* This work was supported by the Helmholtz Association.

* E. Genoyer was supported by a RISE fellowship from the German Academic Exchange Service (DAAD, PKZ: A/12/07058).

TABLES

Table 1. **Primer used for qRT-PCR.**

Gene	*Forward primer (5'- 3')*	*Reverse primer (5'- 3')*
human claudin-4 (CLD4)	TCCTGACTCACGGTGCAAAG	CGTAGGATTCCAAGCGCTG
human claudin-6 (CLD6)	TGCAGCTCCTTCAACCTCG	GTGTCAGGACGACTCCCAGG
human cytochrom P450-1A1 (CYP1A1)	ATGGTCAGAGCATGTCCTTCAGC	TGGGTCAGAGGCAATGGAGAAACT
human E-cadherin (CDH1)	AACAGGATGGCTGAAGGTGACAGA	AACTGCATTCCCGTTGGATGACAC
human fibronectin 1	CCGACCAGAAGTTTGGGTTCT	CAATGCGGTACATGACCCCT
human HPRT	AAGGACCCCACGAAGTGTTG	GGCTTTGTATTTTGCTTTTCCA
human occludin (OCLN)	AACCCAACTGCTCAGTCTTC	TGATCCACGTAGAGTCCAGTAG
human SNAIL homolog 1 (SNAI1/SNAIL)	TGTCAGATGAGGACAGTGGGAA	GCCTCCAAGGAAGAGACTGAAGTA
human zonula occludens-1 (ZO-1)	CAGCCGGTCACGATCTCCT	TCCGGAGACTGCCATTGC
human zonula occludens-2 (ZO-2)	TTGAAGACACGGACGGTGAA	GTGATGGACGACACCAGCG
mouse HPRT	CCTAAGATGAGCGCAAGTTGAA	CCACAGGACTAGAACACCTGCTAAT
mouse zonula occludens-1 (ZO-1)	CAGCCGGTCACGATCTCCT	CCGGAGACTGCCATTGC

AJRCMB Articles in Press. Published on 20-December-2013 as 10.1165/rcmb.2013-0090OC

FIGURE LEGENDS

***Figure 1.*CSE affects cell viability and epithelial resistance of 16HBE14o$^-$ cells.** (A) MTT assay of subconfluent 16HBE14o$^-$ cells treated every 24 hours with 0% - 100% CSE for up to 72 hours. Data were normalized to time-matched controls and represent mean ± SD of three independent experiments. For statistical analysis, Student's *t*-test was used vs. control. (B) Cell morphology of 16HBE14o$^-$ cells treated with indicated concentrations of CSE for 24 hours. Representative bright field images are shown in 100x magnification. (C) Analysis of TEER from 16HBE14o$^-$ cells after exposure to 0% (NT), 10% or 25% CSE for up to 6 hours. Data were normalized to pre-treatment TEER values (518 ± 56 Ω) and represent mean ± SD of four independent experiments. For statistical analysis, one-way ANOVA was used. For all experiments: *p<0.05, **p<0.01, ***p<0.001.

***Figure 2.*Short-term exposure to CSE disrupts tight junctions in 16HBE14o$^-$ cells.** (A) Western blot analysis of protein extracts from 16HBE14o$^-$ cells non-treated (NT) or treated with 10% CSE for 2 and 24 hours. Representative blots of different tight junction proteins with representative β-actin as a loading control are shown. Duplicates of each condition were loaded onto the gels. (B) Protein levels were quantified using Image Lab software (Bio-Rad; Hercules, CA). Data are depicted as mean ± SD of independent experiments relative to β-actin; n = 11-15 (2 hours) and n = 6-9 (24 hours); Student's *t*-test vs. NT: *p<0.05, **p<0.01, ***p<0.001. (C) Indirect immunofluorescence analysis of 16HBE14o$^-$ cells non-treated (NT) or treated with 10% CSE for 72 hours (treatment every 24 hours). Representative ZO-1, ZO-2, and OCLN staining is shown in green and DAPI staining in blue. Scale bar: 50 µm. White arrows indicate disrupted tight junctions between the cells upon CSE exposure. (D) Cells were non-treated (NT) or treated with 10% CSE for 2 hours, cytoplasmic and membrane proteins were fractionated and analyzed via western blot analysis. Na^+/K^+-ATPase and GAPDH represent markers for membrane and cytoplasmic fractions, respectively. Representative blots are shown and densitometry analysis of membrane bound ZO-1 was performed using Image Lab software. Data are depicted as mean ± SD of three independent experiments relative to Na^+/K^+-ATPase; Student's *t*-test vs. NT: ***p<0.001.

***Figure 3.*ZO-1 is downregulated in smoke exposed bronchi from mice.** (A) qRT-PCR analysis of expression levels of ZO-1 mRNA. Mouse bronchi were *ex vivo* treated with 5%, 10% or 20% CSE for 6 and 24 hours and values depict mean ± SD relative to time-matched controls with n = 3 per group; Student's *t*-test vs. controls: *p<0.05, **p<0.01, ***p<0.001. (B) Paraffin sections from control (NT) and smoke exposed bronchi for 24

hours are shown in two different magnifications; scale bars = 40 µm (upper panel) and 20 µm (lower panel). Representative ZO-1 immunostaining is shown in red and DAPI staining in blue. White arrows indicate intact tight junctions in control bronchi.

Figure 4. **Short-term exposure of 16HBE14o- cells to TGF-β1 prevents CSE induced downregulation of ZO-1 and ZO-2.**(A) Western blot analysis of protein extracts from 16HBE14o- cells non-treated (NT) or treated with TGF-β1 (0.1-10 ng/ml) for 24 hours. Representative blots of tight junction proteins with corresponding β-actin as a loading control are shown, pSmad3 served as a marker for the TGF-β1 response. (B) Western blot analysis of protein extracts from 16HBE14o- cells non-treated (NT) or treated with TGF-β1 (5ng/ml), 2.5% CSE, 10% CSE alone or in combination for 2 and 24 hours. Representative blots of different tight junction proteins with corresponding β-actin as a loading control are shown. (C) Indirect immunofluorescence analysis of 16HBE14o- cells treated with 10% CSE or 10% CSE + TGF-β1 (5 ng/ml) for 72 hours (treatment every 24 hours). Representative ZO-1 and ZO-2 staining is shown in green and DAPI staining in blue. Scale bar: 50 µm. White arrows indicate preserved tight junctions between the cells upon TGF-β1 exposure. (D), (E) Analysis of TEER from 16HBE14o$^-$ cells (cultured on: collagen type I (D); collagen type IV (E)) after exposure to TGF-β1 (5 ng/ml), 10% CSE, 25% CSE alone or in combination for 6 hours. Data were normalized to pre-treatment TEER values and untreated control. Data of three independent experiments with median ± quartile are shown. For statistical analysis, Student's t-test was used. For all experiments: *p<0.05, **p<0.01, ***p<0.001.

Figure 5.**Long-term exposure of 16HBE14o$^-$ cells to TGF-β1 protects CSE-induced loss of tight junction components.** qRT-PCR analysis of expression levels of ZO-1, ZO-2, OCLN, CLD4 and CLD6 mRNA relative to controls. Cells were treated long-term (every 24 hours for 7 times and split once in between) with TGF-β1 (5 ng/ml), 2.5% CSE, 10% CSE or in combination. Values are depicted as mean ± SD of three independent experiments; Student's *t*-test vs. controls: *p<0.05, **p<0.01, ***p<0.001.

Figure 6. **pHBECs at air-liquid-interface differentiate into a mucociliary epithelium.**(A) Indirect immunofluorescence analysis of 7, 14, and 21 days differentiated pHBECs. Representative acTubulin (acetylated tubulin), CC10 (clara cell specific protein), Muc5AC (mucin 5A/C) and ZO-1 staining is shown in green or red, as depicted, and DAPI staining in blue. Scale bar: 50 µm. (B). Data are depicted as mean ± SEM of independent differentiations relative to total number of cells. n = 10 images per group were analyzed.

AJRCMB Articles in Press. Published on 20-December-2013 as 10.1165/rcmb.2013-0090OC

Figure 7. **TGF-β1 exerts protective effects in primary bronchial epithelial cells exposed to CSE.** (A)Western blot analysis of protein extracts from non-differentiated pHBECs non-treated (NT) or treated for 24 hours with CSE (5% - 25%) (left panel), with TGF-β1 (0.1 - 5 ng/ml) (middle panel), or with 10% CSE, TGF-β1 (ng/ml) or 10% CSE + TGF-β1 (5 ng/ml) (right panel). Representative blots of ZO-1, ZO-2, and pSmad3 with representative β-actin as a loading control are shown. (B) Western blot analysis of protein extracts from differentiated pHBECsnon-treated (NT) or treated for 72 hours with CSE (5% - 25%) (left panel), with TGF-β1 (0.1 - 5 ng/ml) (middle panel), or with 10% CSE, TGF-β1 (ng/ml) or 10% CSE + TGF-β1 (5 ng/ml) (right panel). Representative blots of ZO-1, ZO-2, and pSmad3 with representative β-actin as a loading control are shown. (C) Indirect immunofluorescence analysis of 7 (left panel), or 14 days (right panel) differentiated pHBECs exposed to 10% CSE for 72 hours (treatment every 24 hours). Representative ZO-1 staining is shown in red, Muc5AC staining in green, and DAPI staining in blue. Scale bar: 50 μm. White arrows indicate disrupted or zipper-like junctions between the cells upon CSE exposure. (D) Analysis of TEER from differentiated pHBECs after exposure to TGF-β1 (5 ng/ml), 10% CSE, 25% CSE alone or in combination for 6 hours. Data were normalized to pre-treatment TEER values. Data of independent pHBEC differentiations with median ± quartile are shown. For statistical analysis, Student's t-test was used: *$p<0.05$, **$p<0.01$.

Figure 1

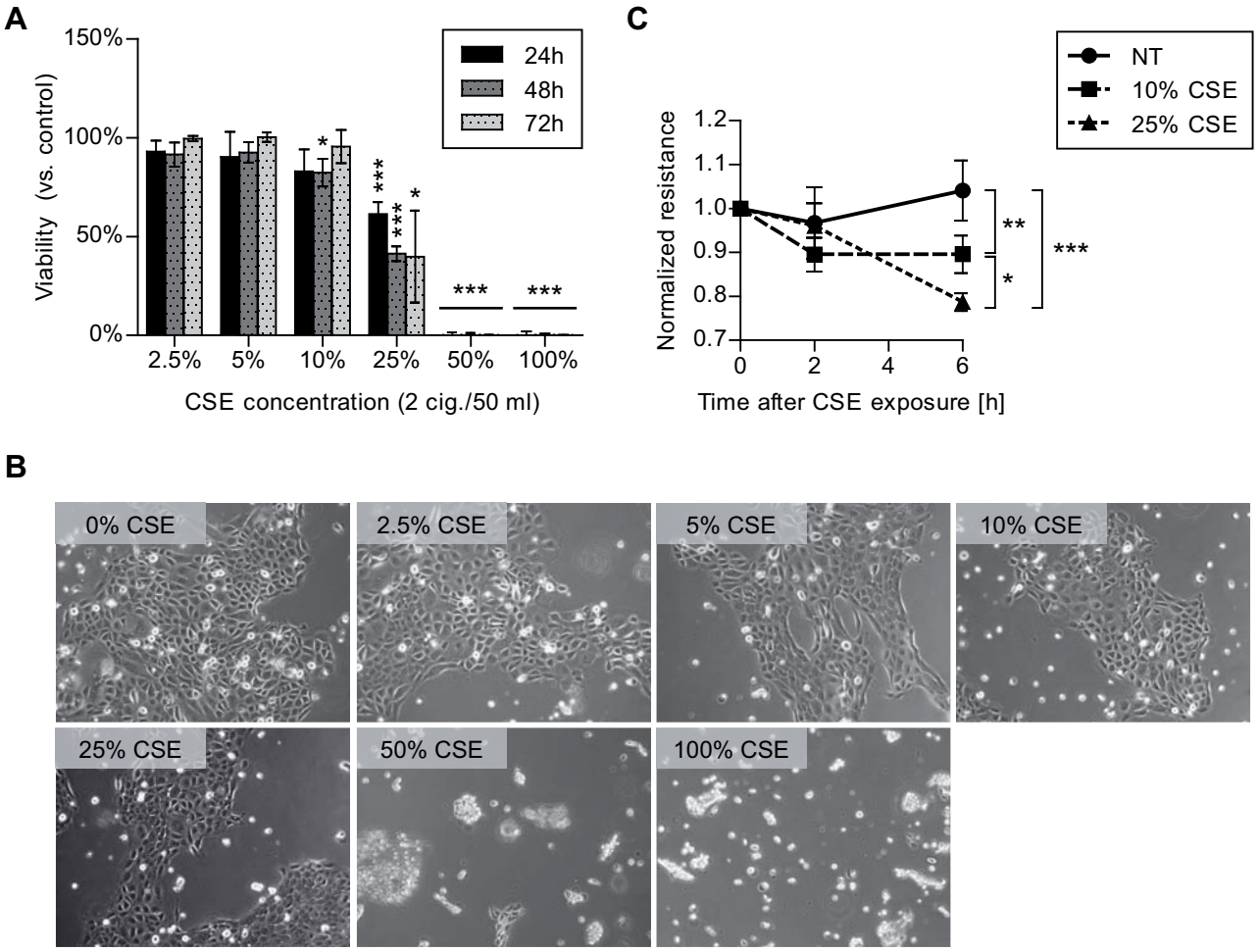

AJRCMB Articles in Press. Published on 20-December-2013 as 10.1165/rcmb.2013-0090OC

Figure 2

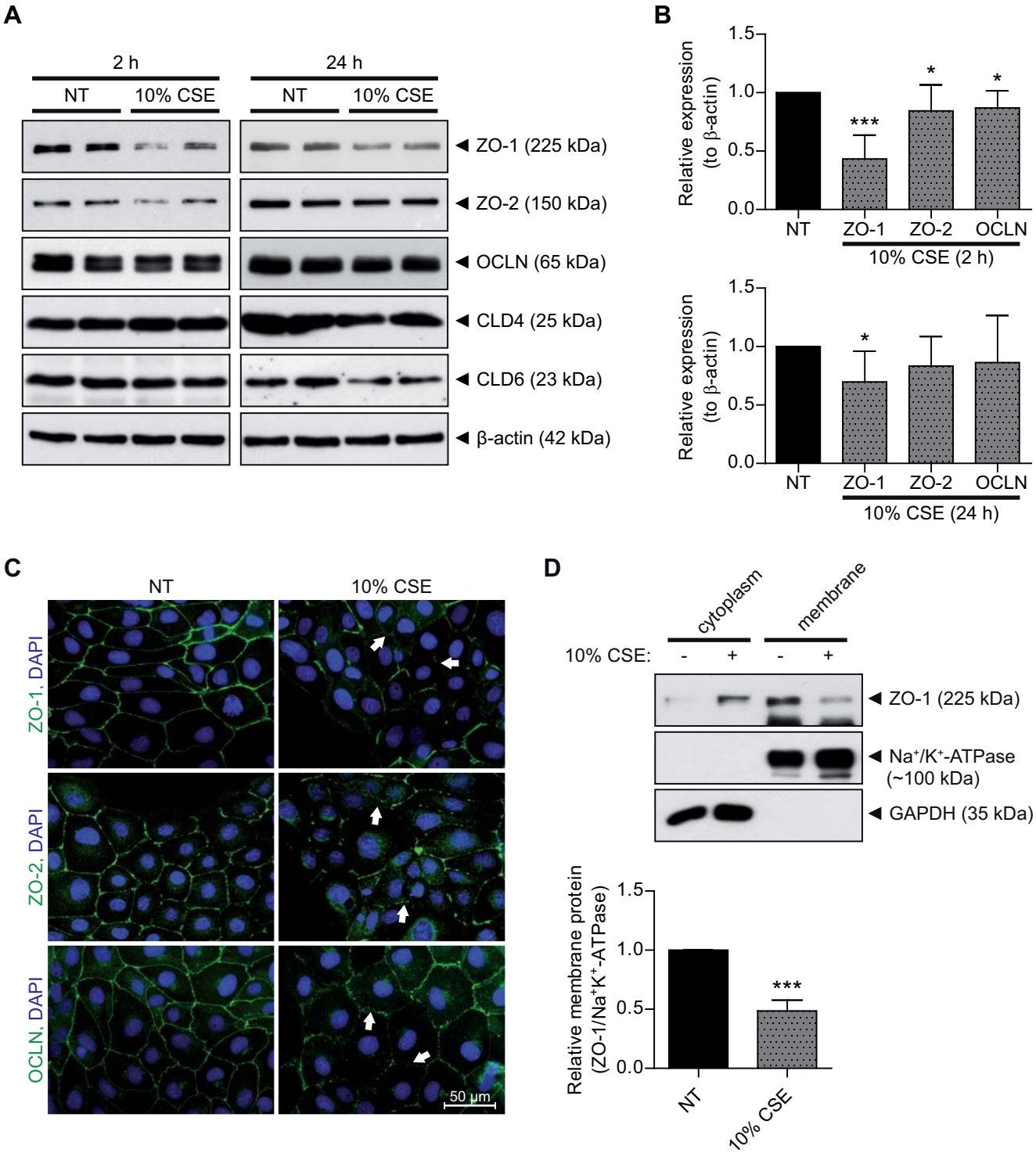

Figure 3

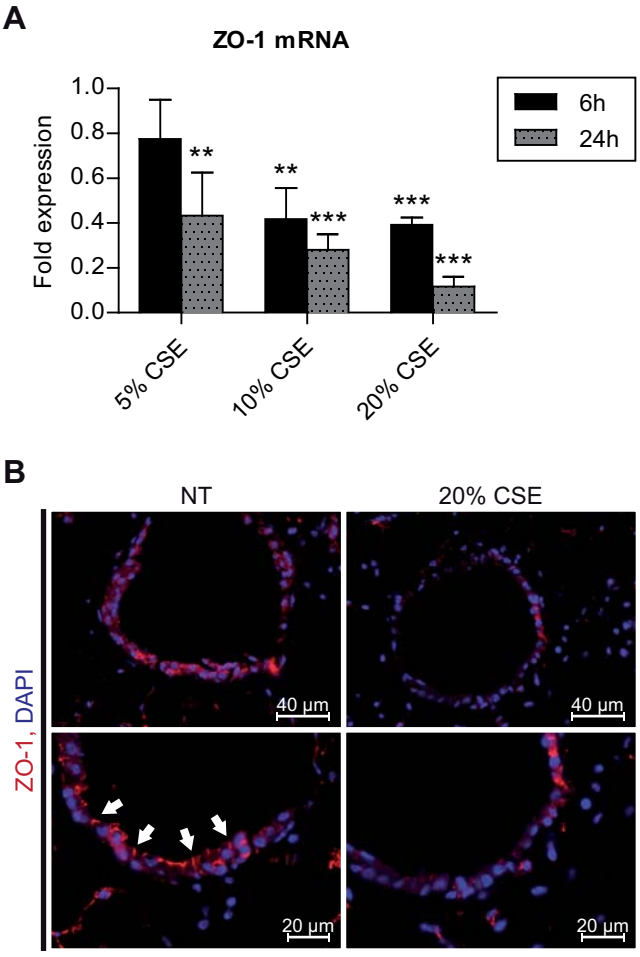

AJRCMB Articles in Press. Published on 20-December-2013 as 10.1165/rcmb.2013-0090OC

Figure 4

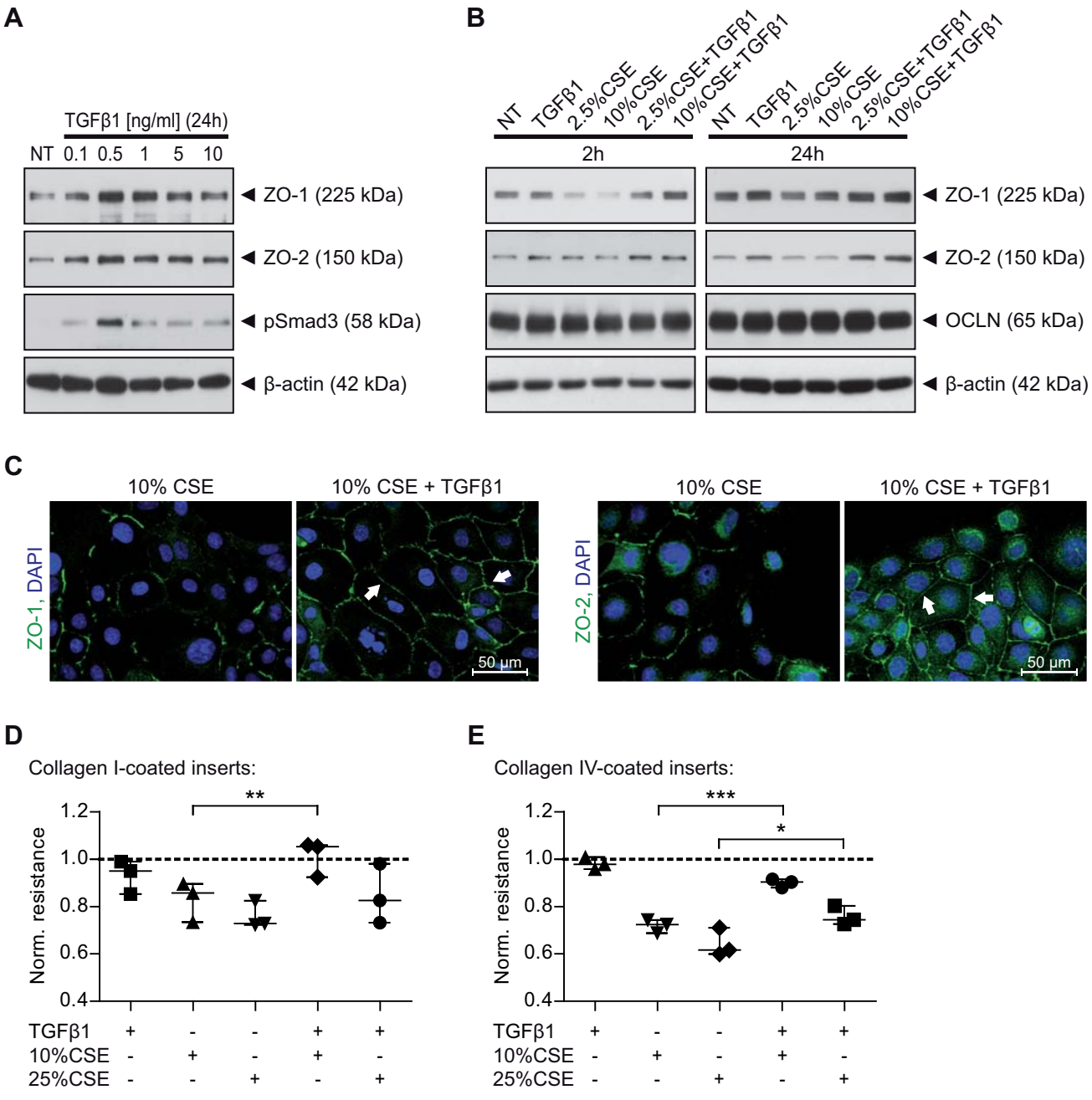

Figure 5

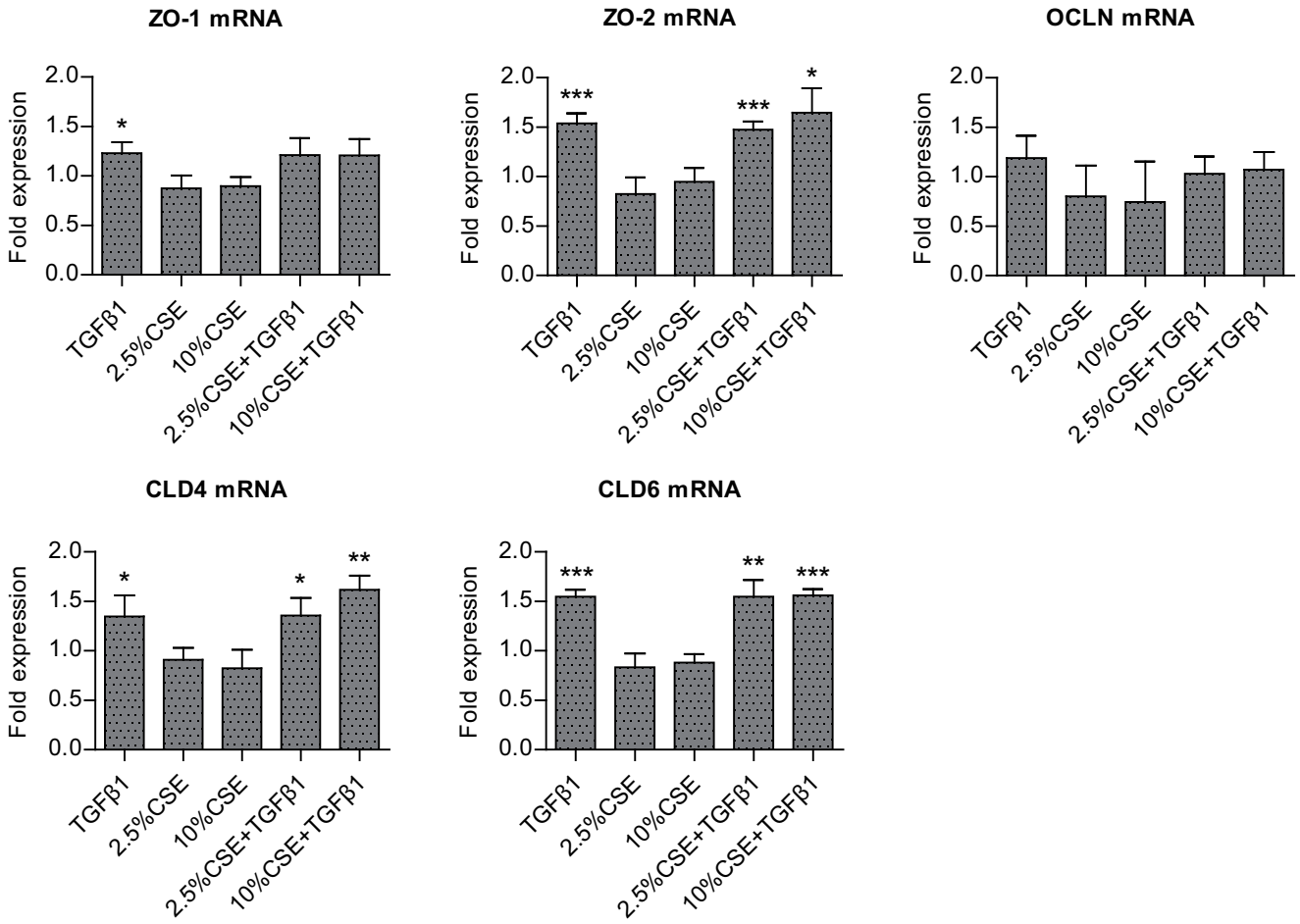

AJRCMB Articles in Press. Published on 20-December-2013 as 10.1165/rcmb.2013-0090OC

Figure 6

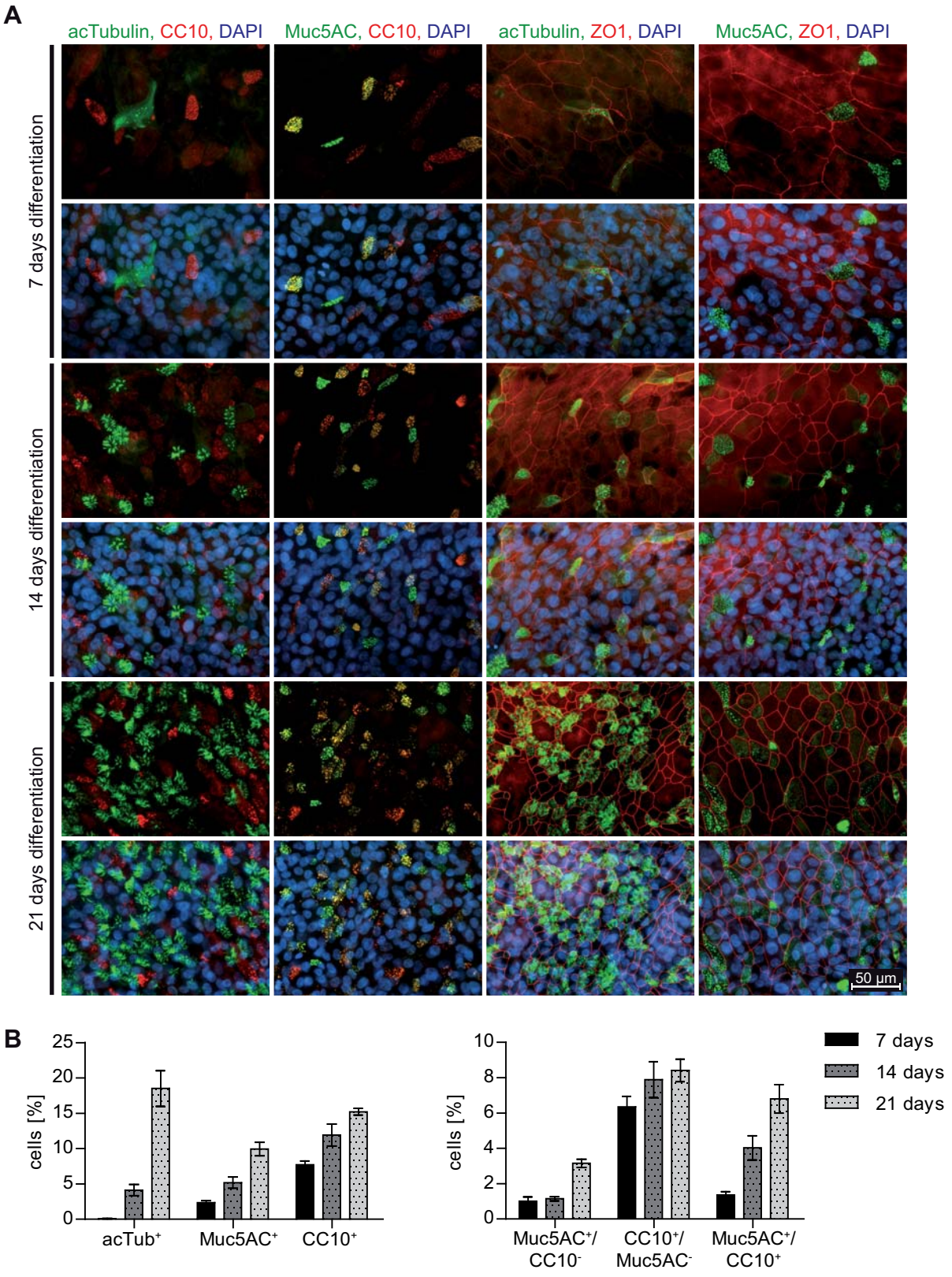

Figure 7

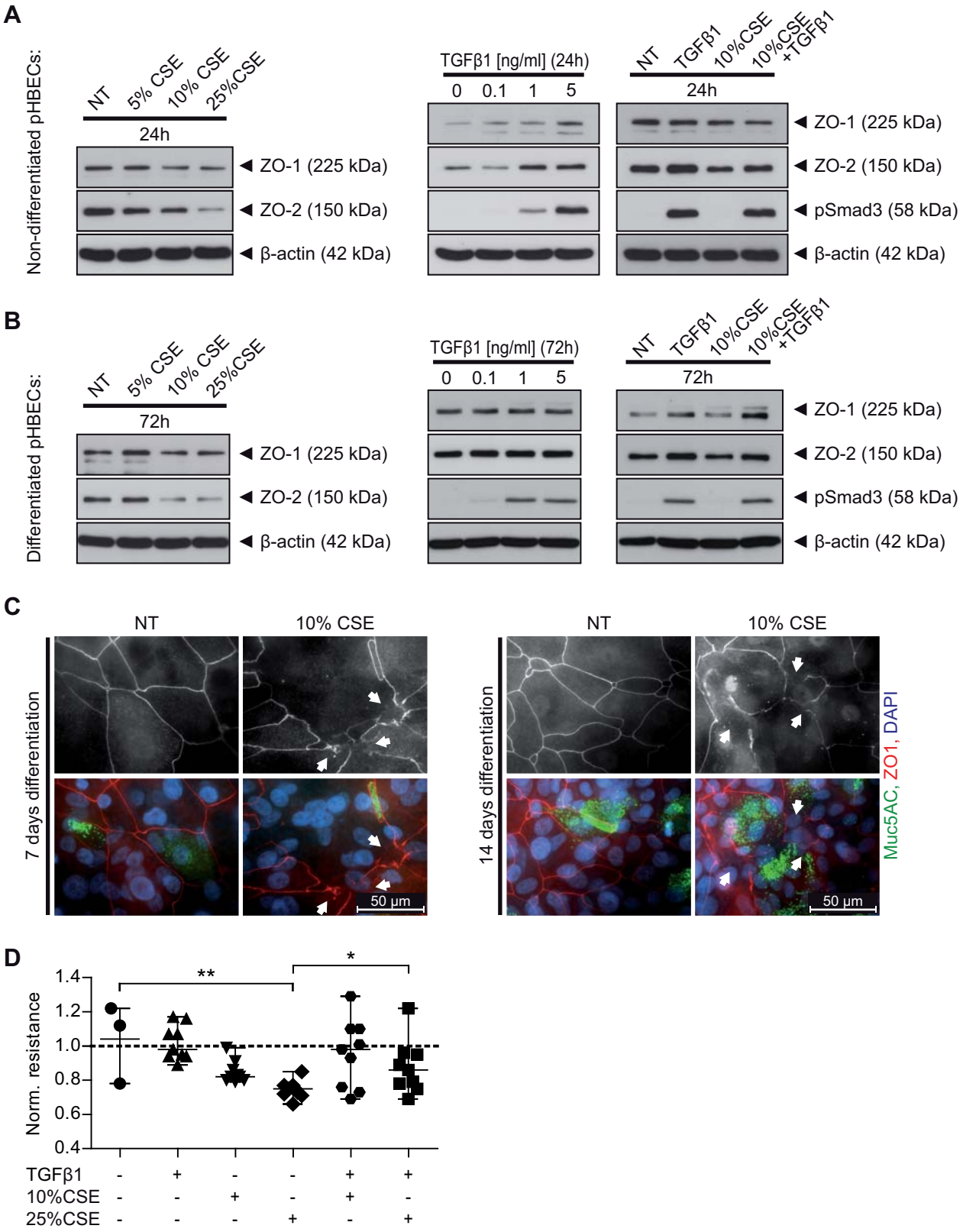

AJRCMB Articles in Press. Published on 20-December-2013 as 10.1165/rcmb.2013-0090OC

ONLINE DATA SUPPLEMENT

Cigarette Smoke-Induced Disruption of Bronchial Epithelial Tight Junctions is Prevented by Transforming Growth Factor-Beta

Andrea C. Schamberger, Nikica Mise, Jie Jia, Emmanuelle Genoyer,

Ali Ö. Yildirim, Silke Meiners, and Oliver Eickelberg

MATERIAL AND METHODS

Preparation of CSE

100% CSE was generated as previously described (1). Briefly, mainstream smoke of Kentucky 3RF4 research cigarettes with filter (Lexington, KY) was bubbled through cell culture media in a closed environment with limited air flow. The burning time per cigarette was about 4 minutes. For 16HBE14o- cells, smoke of two cigarettes was bubbled through 50 ml MEM media. The obtained media was considered as 100% CSE. CSE was sterile filtrated, aliquoted, and stored at -80°C. For usage, CSE was quickly thawed, supplemented with FBS (final: 10%) and diluted with MEM to the indicated concentration. For human primary bronchial epithelial cells, smoke of three Kentucky 3RF4 research cigarettes was bubbled through 50 ml of BEBM media (Lonza) with a flow rate of 0.3 liter/minute. CSE for primary cells was diluted in BEGM media to the indicated concentrations. Both extract were tested via several viability assays, resulting in comparable non-toxic doses for 16HBE14o- cells or human primary bronchial cells. CSE activity was routinely monitored via its capability to induce cytochrome P450-1A1.

Cell Fractionation and Western Blot Analysis

To obtain proteins from cytoplasmic and membrane fractions, cells on 10 cm plates were washed twice with ice-cold PBS and scraped in ice-cold subcellular fractionation buffer (250 mM Sucrose, 20 mM HEPES pH 7.4, 10 mM KCl, 1.5 mM $MgCl_2$, 1 mM EDTA, 1 mM EGTA, 1 mM DTT) supplemented with Complete^{TM} protease inhibitor cocktail (Roche; Mannheim, Germany) and PhosSTOP phosphatase inhibitor cocktail (Roche). Cell lysates were passed through a needle (25 G, 10 times), chilled on ice for 20 minutes and centrifuged at 720 G for 5 minutes (4°C). To clear the supernatant further, it was re-centrifuged at 10,000 G for 10 minutes (4°C). The supernatant was ultra-centrifuged at 100,000 G for 1 hour (4°C), resulting in the cytoplasmic (supernatant) and membrane fraction (pellet) which was lysed in RIPA buffer supplemented with Complete^{TM} protease inhibitor cocktail and PhosSTOP phosphatase inhibitor cocktail. Membrane lysates were passed through a needle (25 G, 10 times) and sonified using a ultrasonic homogenizer (Bandelin; Berlin, Germany) (10% power, 10 times).

Whole cell lysates were obtained using RIPA buffer (50 mM Tris·HCl, pH 7.6, 150 mM NaCl, 1% Nonidet P-40, 0.5% sodium deoxycholate, and 0.1% SDS) supplemented with CompleteTM protease inhibitor cocktail and PhosSTOP phosphatase inhibitor cocktail. Equal amounts of protein (20 - 30 µg) were subjected to SDS-PAGE and standard western blot techniques were performed as described previously (2). The following antibodies were used: anti-OCLN (#71-1500) and anti-ZO-1 (#40-2200) from Invitrogen (Paisley, UK), anti-GAPDH (14C10)

AJRCMB Articles in Press. Published on 20-December-2013 as 10.1165/rcmb.2013-0090OC

(#2118) and anti-ZO-2 (#2847) from Cell Signaling (Danvers, MA), anti-CLD4 (C18) (sc-17664) and anti-Na^+/K^+-ATPase α (H3) (sc-48345) from Santa Cruz (Santa Cruz, CA), anti-CLD6 (ab107059) from Abcam (Cambridge, MA), anti-β-actin (A3854) from Sigma-Aldrich and anti-pSmad3 (#04-1042) from Millipore (Billerica, MA).

RNA Isolation and Quantitative Real-Time PCR (qRT-PCR) Analysis

Total RNA isolation, reverse transcription, and qRT-PCR was performed as previously described (2). For airway RNA, frozen tissue was homogenized and RNA isolated using innuPREP-Micro-RNA-Kit (Analytik Jena; Jena, Germany). For specific gene amplification, primers listed in Table 1 in the main manuscript were used. HPRT was used as a housekeeping gene for standardization of relative mRNA expression.

MTT Cytotoxicity Assay

To assess cytotoxicity of CSE, $1x10^4$ cells/cm^2 were seeded in 24-well plates and treated with CSE. After 24, 48, and 72 hours, Thiazolyl-Blue-Tetrazolium-Bromide (Sigma-Aldrich) in PBS was added to each well (final: 0.5 mg/ml) and incubated for 1 hour at 37°C. The supernatant was aspirated and crystals were dissolved in isopropanol/0.1% Triton X-100. Absorbance (570 nm) was measured using the Sunrise multiplate reader (Tecan; Männedorf, Switzerland).

LDH Cytotoxicity Assay

To assess cytotoxicity of CSE and TGF-β1 on confluent cells, activity of released lactate dehydrogenase (LDH) was measured using the Cytotoxicity Detection Kit (LDH) (Roche) according to the manufacturer's instructions. Briefly, supernatants of untreated (= low control) and treated cells were stored at 4°C until analysis the next day. For maximal LDH release (= high control), untreated cells were lysed with 2% Triton X-100/ media/0% FCS for 15 min (RT). Cell debris were centrifuged out with 250 g for 10 min (4°C). Samples were mixed with equal amounts of substrate mixture and incubated for 30 min (RT) in the dark. Absorbance (490 nm) was measured using the Sunrise multiplate reader, background values subtracted and cytotoxicity calculated using the formula: $Cytotoxicity\ (\%) = \frac{experimental\ value - low\ control}{high\ control - low\ control} \times 100$.

Dead Cell Assay with Annexin V and PI

To assay for apoptotic and necrotic cells upon CSE and TGF-β1 exposure, cells were double stained with fluorescein isothiocyanate (FITC) annexin V (BD Biosciences; Heidelberg, Germany) and propidium iodide (PI)

staining solution (BD Biosciences). $2x10^4$ cells/cm^2 were seeded in 60-mm dishes and treated with CSE and TGF-β1 for 24 and 72 hours. According the manufacturer's instructions, cells were washed with PBS, trypsinized and resuspended in binding buffer (10 mM HEPES, 140 mM NaCl, and 2.5 mM CaCl2, pH 7.4). Cells were stained with FITC annexin V and PI for 15 minutes at RT and analyzed by flow cytometry (BD LSRII) within one hour. Data analysis was performed using FlowJo software (version 7.6.5).

BrdU Proliferation Assay

To assess influence of CSE and TGF-β1 on cell proliferation, BrdU Cell Proliferation Assay Kit (Cell Signaling) was used according the manufacturer's instructions. Briefly, $2x10^4$ cells/cm^2 were seeded in 96-well plates and treated with CSE and TGF-β1. After 24 and 72 hours, 5-bromo-2'-deoxyuridine (BrdU) solution was added to each well (final: 1x) and incubated for 2 hours at 37°C. Cell supernatants were aspirated and cells fixed for 30 min at RT. BrdU detection antibody was allowed to bind for 1 hour, cells were washed and HRP-conjugated secondary antibody was added for 30 min at RT. After final washing, HRP substrate TMB was added for 30 minutes. Stop solution was added and absorbance (450 nm) was measured using the Sunrise multiplate reader (Tecan).

AJRCMB Articles in Press. Published on 20-December-2013 as 10.1165/rcmb.2013-0090OC

FIGURE LEDGENDS

Figure E1. **Confluent 16HBE14o$^-$ with high resistance to CSE**. Analysis of LDH assay performed with confluent 16HBE14o$^-$ cells after exposure to 10% and 25% CSE for 6 hours. Data were normalized to time-matched negative controls (non-treated cells) and positive controls (maximal LDH activity measured in non-treated lysed cells). (A) Cytotoxicity. (B) Viability. Data are depicted as mean ± SD of three independent experiments.

Figure E2. **Short-term exposure of 16HBE14o- cells to TGF-β1 and CSE does not alter transcript levels of junctional components.** qRT-PCR analysis of expression levels of ZO-1, ZO-2, OCLN and CDH1 (E-cadherin) mRNA relative to controls. Cells were treated with TGF-β1 (5 ng/ml), 2.5% CSE, 10% CSE or in combination for 2 and 24 hours. Values are depicted as mean ± SD of three independent experiments; Student's t-test vs. controls: *$p<0.05$.

Figure E3. **TGF-β1 decreases proliferation but does not alter cell survival.** (A) Cell proliferation was measured with a BrdU incorporation assay. 16HBE14o- cells were treated with TGF-β1 (5 ng/ml), 10% CSE or in combination for 24 and 72 hours. Data are depicted as mean ± SD of three independent experiments performed in duplicates; Student's *t*-test vs. controls: *$p<0.05$, ***$p<0.001$. (B) Fluorescence-activated cell sorter analysis of cells double stained with annexin V-fluorescein isothiocyanate (FITC) and propidium iodide (PI) to assay for apoptotic and necrotic cells. 16HBE14o- cells were treated with TGF-β1 (5 ng/ml), 10% CSE, 25% CSE or in combination for 24 and 72 hours. Unstained cells were used for cell gating and negative Annexin V-FITC control. Single Annexin V-FITC staining of cells and single PI staining of permeabilized cells served as positive controls. Representative scatter plots of three independent experiments are shown: lower right quarter – early apoptosis, upper left quarter – necrosis, upper right quarter – late apoptosis/ necrosis.

Figure E4. **Long-term treatment of 16HBE14o$^-$ cells with TGF-β1 induces mesenchymal markers.** (A) Treatment scheme of chronically treated 16HBE14o$^-$ cells: Cells were retreated every 24 hours for 7 days and split once in between without treatment. (B) qRT-PCR analysis of expression levels of fibronectin, SNAIL and CDH1 (E-cadherin) mRNA relative to controls. Cells were treated chronically with TGF-β1 (5 ng/ml), 2.5% CSE, 10% CSE or in combination. Values are depicted as mean ± SD of three independent experiments; Student's *t*-test vs. controls: *$p<0.05$, **$p<0.01$, ***$p<0.001$.

Figure E5. **CSE but not TGF-β1 affects cell viability in human primary bronchial epithelial cells.** Analysis of LDH assay performed with primary bronchial epithelial cells. Left panel: Cells were treated every 24 hours with 0% - 50% CSE for up to 72 hours. Right panel: Cells were treated every 24 hours with TGF-β1 (5 ng/ml), 10% CSE or in combination for up to 72 hours. (A) Primary bronchial epithelial cells cultured on plastic. (B) Differentiated primary bronchial epithelial cells cultured on air-liquid interface for 14 days. Data were normalized to time-matched negative controls (non-treated cells) and positive controls (maximal LDH activity measured in non-treated lysed cells). Data are depicted cumulative as mean ± SD of independent experiments.

Figure E6. **Differentiated pHBECs show features of a polarized, multilayered epithelium.** Indirect immunofluorescence analysis of differentiated pHBECs. Representative acTubulin (acetylated tubulin), CC10 (clara cell specific protein), Muc5AC (mucin 5A/C) and p63 staining is shown in green or red, as depicted, and DAPI staining in blue. Scale bar: 50 μm. White arrows indicate apical localization of acetylated tubulin, CC10, and Muc5AC, and basal localization of p63.

AJRCMB Articles in Press. Published on 20-December-2013 as 10.1165/rcmb.2013-0090OC

Figure E1

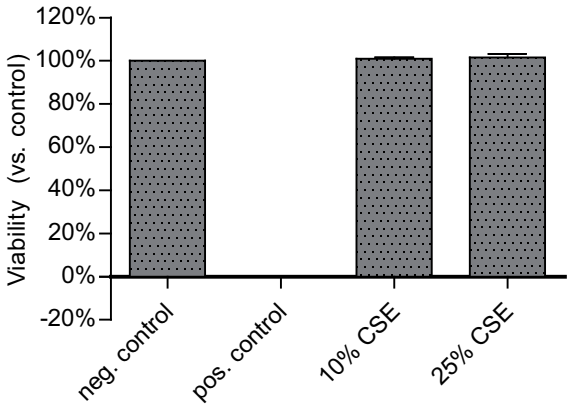

Figure E2

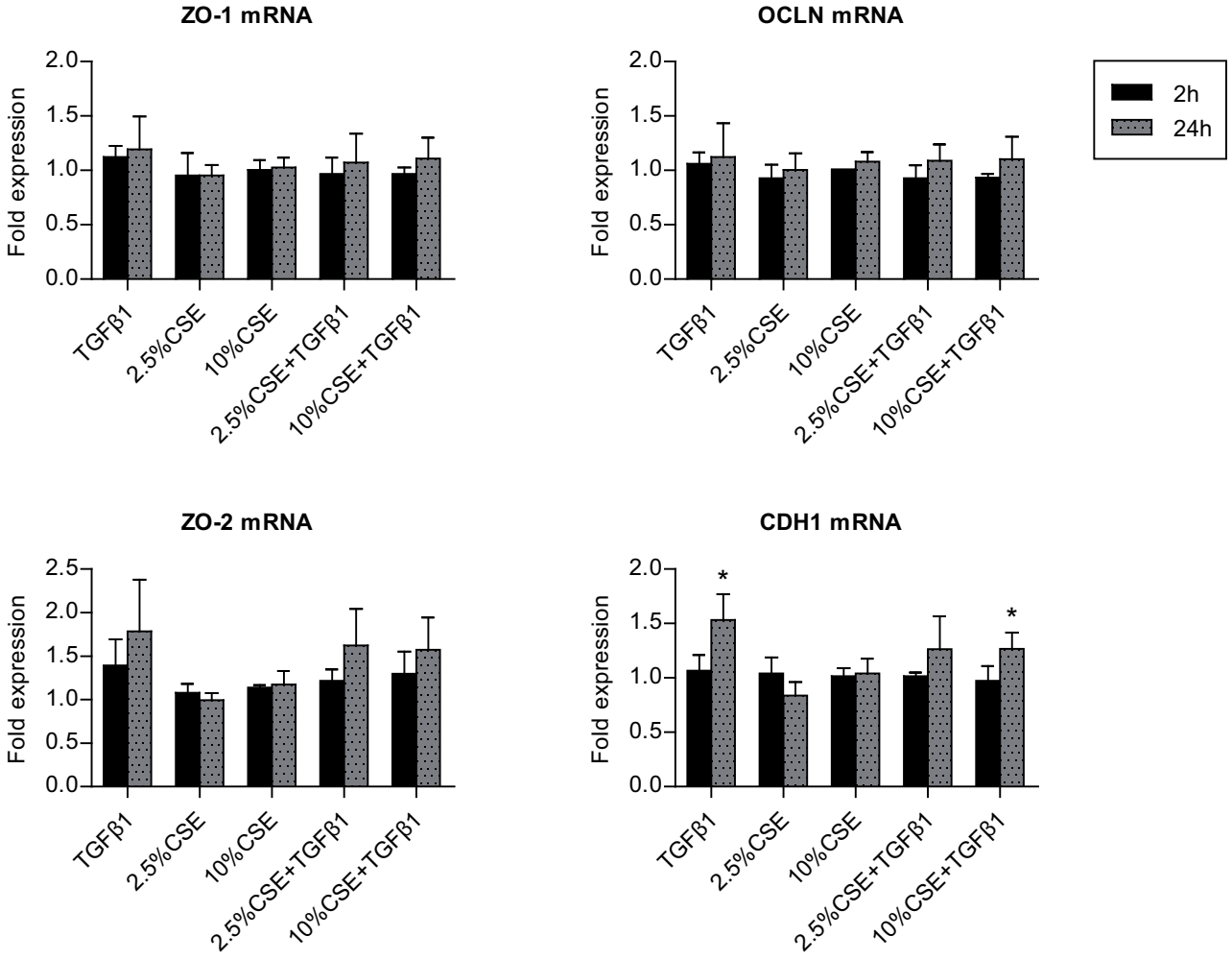

AJRCMB Articles in Press. Published on 20-December-2013 as 10.1165/rcmb.2013-0090OC

Figure E3

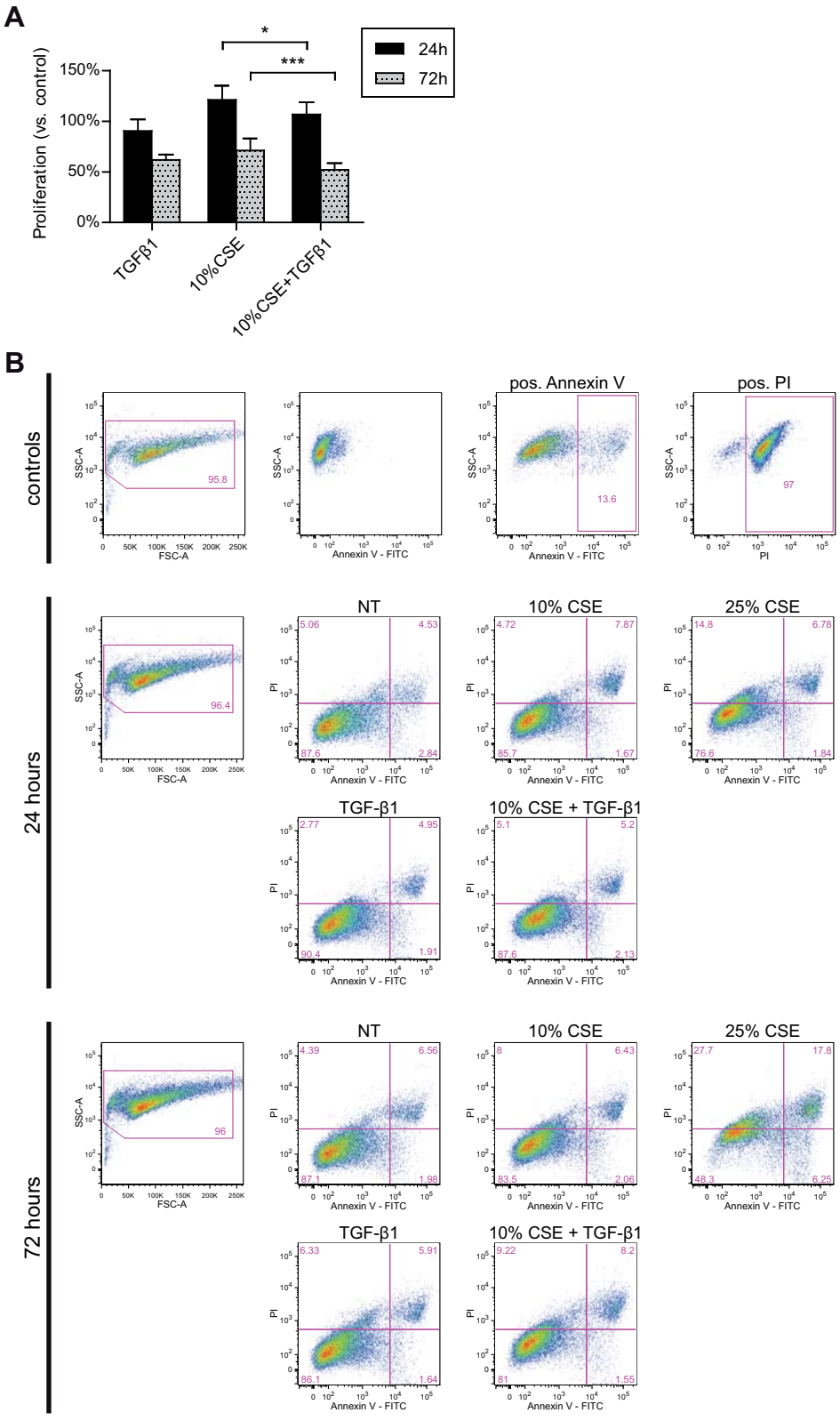

Figure E4

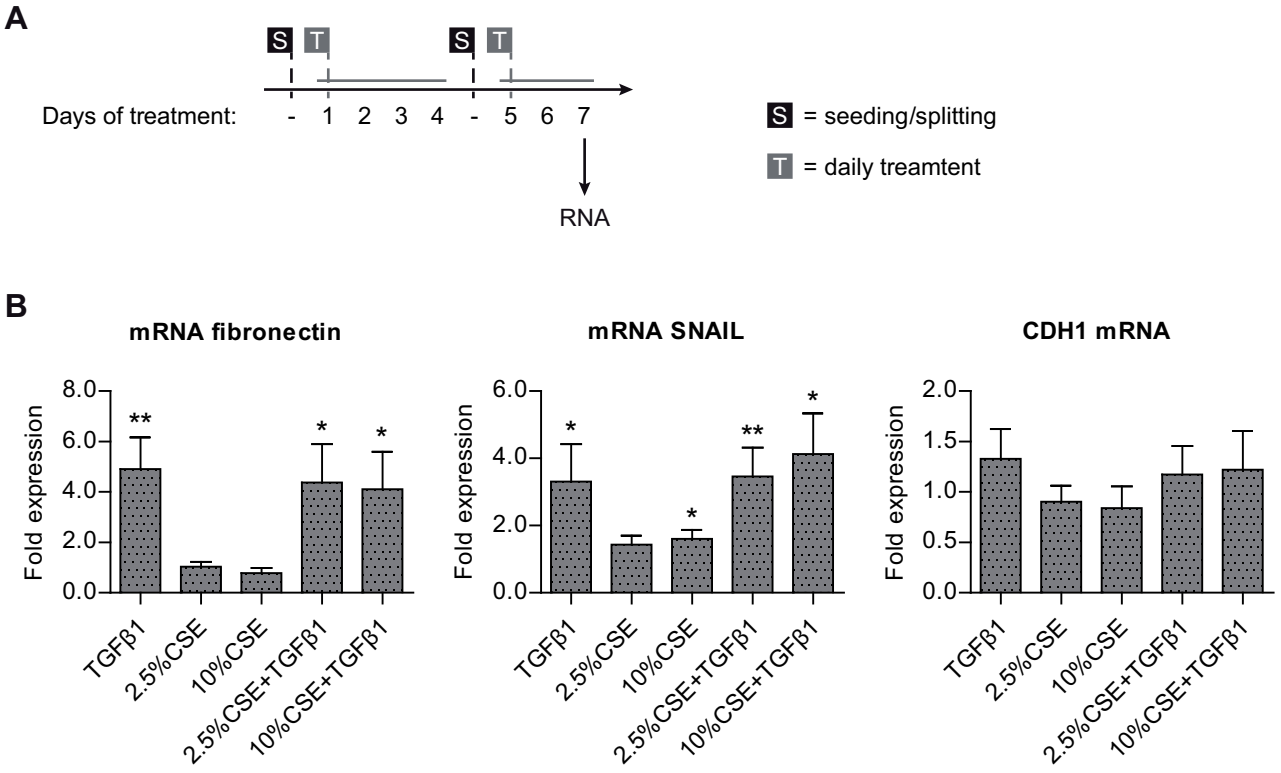

AJRCMB Articles in Press. Published on 20-December-2013 as 10.1165/rcmb.2013-0090OC

Figure E5

A

Non-differentiated pHBECs:

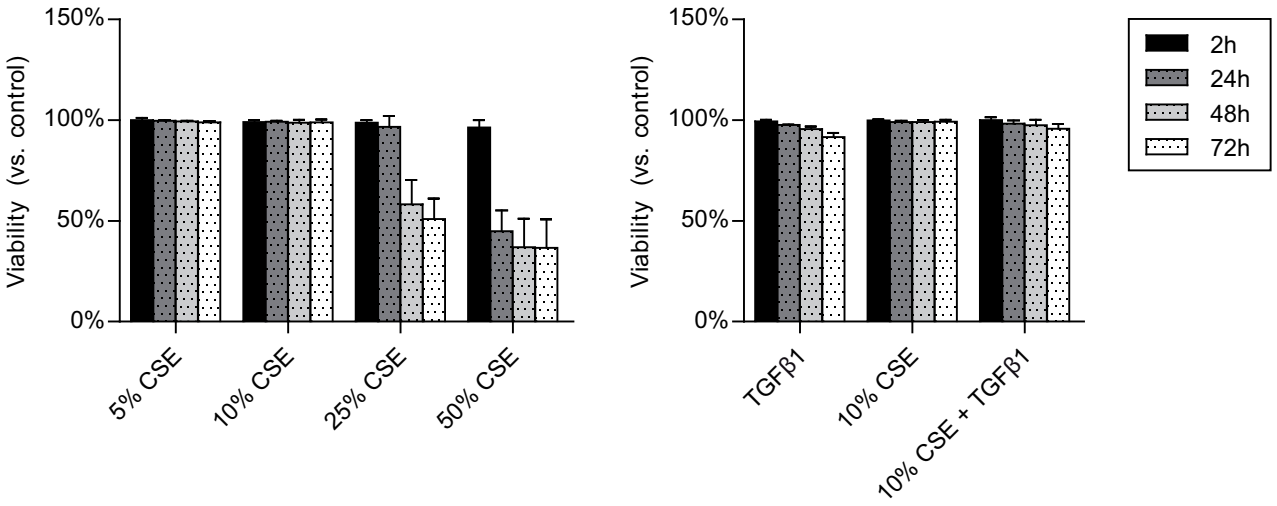

B

Differentiated pHBECs:

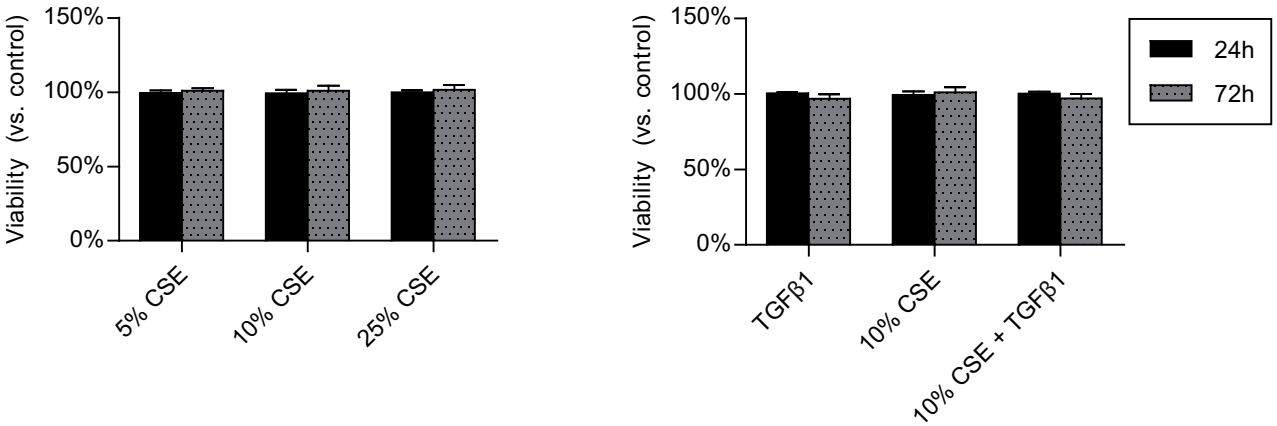

Figure E6